



1 Estimation of mechanistic parameters in the gas-phase reactions of 2 ozone with alkenes for use in automated mechanism construction

3 Mike J. Newland^{1,a}, Camille Mouchel-Vallon^{1,b}, Richard Valorso², Bernard Aumont², Luc
4 Vereecken³, Michael E. Jenkin⁴, Andrew R. Rickard^{1,5}

5 ¹ Wolfson Atmospheric Chemistry Laboratories, Department of Chemistry, University of York, United Kingdom

6 ² Univ Paris Est Creteil and Université de Paris, CNRS, LISA, F-94010 Créteil, France.

7 ³ Forschungszentrum Jülich GmbH, Institute for Energy and Climate, IEK-8 Troposphere, 52428 Jülich, Germany

8 ⁴ Atmospheric Chemistry Services, Okehampton, Devon, EX20 4QB, United Kingdom.

9 ⁵ National Centre for Atmospheric Science, Wolfson Atmospheric Chemistry Laboratories, University of York,
10 United Kingdom.

11

12 ^a now at: ICARE-CNRS, 1 C Av. de la Recherche Scientifique, 45071 Orléans Cedex 2, France.

13 ^b now at: Laboratoire d'Aérodologie, Université de Toulouse, CNRS, UPS, Toulouse, France.

14 *Correspondence to:* Mike Newland (mike.newland@gmail.com) and Andrew Rickard
15 (andrew.rickard@york.ac.uk).
16

17 **Abstract.** Reaction with ozone is an important atmospheric removal process for alkenes. The ozonolysis reaction
18 produces carbonyls, and carbonyl oxides (Criegee intermediates, CI), which can rapidly decompose to yield a
19 range of closed shell and radical products, including OH radicals. Consequently, it is essential to accurately
20 represent the complex chemistry of Criegee intermediates in atmospheric models in order to fully understand the
21 impact of alkene ozonolysis on atmospheric composition. A mechanism construction protocol is presented which
22 is suitable for use in automatic mechanism generation. The protocol defines the critical parameters for describing
23 the chemistry following the initial reaction, namely: the primary carbonyl / CI yields from the primary ozonide
24 fragmentation; the amount of stabilisation of the excited CI (CI*); the unimolecular decomposition pathways,
25 rates and products of the CI; the bimolecular rates and products of atmospherically important reactions of the
26 stabilised CI (SCI). This analysis implicitly predicts the yield of OH from the alkene-ozone reaction. A
27 comprehensive database of experimental OH, SCI and carbonyl yields has been collated using reported values in
28 the literature and used to assess the reliability of the protocol. The protocol provides estimates OH, SCI and
29 carbonyl yields with a root mean square error of 0.13 and 0.12 and 0.14, respectively. Areas where new
30 experimental and theoretical data would improve the protocol and its assessment are identified and discussed.

31 1 Introduction

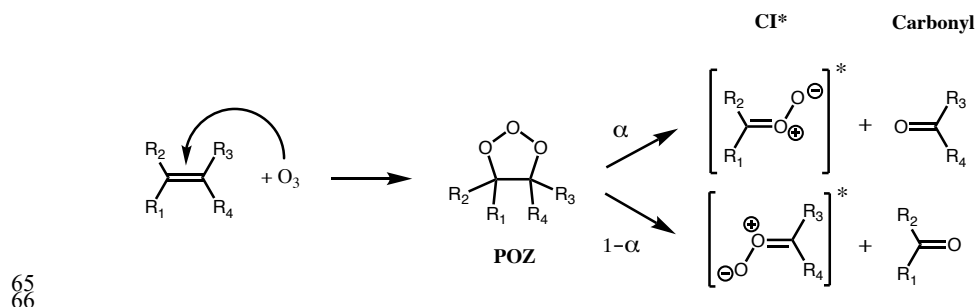
32 Reaction with ozone is an important atmospheric removal process for alkenes, competing with reaction with OH
33 and NO₃ radicals. The ozonolysis reaction produces carbonyls and carbonyl oxides, commonly denoted Criegee
34 intermediates (CI), which can rapidly rearrange or decompose to yield a range of closed shell and radical products
35 (Johnson and Marston, 2008). Alkene ozonolysis has been shown to be an important non-photolytic source of OH
36 radicals, with field measurements (Paulson and Orlando, 1996; Elshorbany et al., 2009) and modelling studies
37 (e.g. Bey et al., 1997) suggesting it to be the dominant tropospheric OH source at night, in the winter (Heard et
38 al., 2004; Emmerson et al., 2005), and in indoor environments (Carshaw, 2007). Unimolecular CI reactions (Ehn
39 et al. 2014; Iyer et al., 2020) and bimolecular reactions of Stabilised Criegee Intermediates (SCI), with e.g. organic
40 acids and peroxy radicals (e.g. Kristensen et al., 2014; Sakamoto et al., 2013; Zhao et al., 2015; Mackenzie-Rae



41 et al., 2016), have been implicated in secondary organic aerosol formation. SCI can also act as an oxidant, this
42 has been studied particularly for the reaction with SO₂ (e.g. Welz et al., 2012, Mauldin II et al., 2012; Caravan et
43 al., 2020) which can lead to sulfate aerosol production and hence impact radiative forcing and climate (Pierce et
44 al. 2013; Percival et al. 2013). However, both the SO₂ and organic acid reactions, while important locally, are
45 likely only of minor importance to global budgets of sulfate aerosol and organic acids (Welz et al., 2014; Newland
46 et al., 2018). The dominant removal processes for most SCI in the troposphere are reaction with water vapour or
47 unimolecular reaction (Vereecken et al., 2017). However, for certain structures, these reactions are sufficiently
48 slow for bimolecular reactions with other trace gases to become important.

49 Understanding of the complex nature of the chemistry of Criegee intermediates has progressed rapidly
50 in recent years, particularly with regard to the mechanisms and rates of decomposition of CI*/SCI, and the
51 bimolecular reaction rates of SCI. This has been facilitated by: direct experimental measurements of CI kinetics,
52 generating CI through photolysis of di-iodo precursors (e.g. Welz et al., 2012; Chhantyal-Pun et al. 2020, and
53 references therein); indirect measurements of CI kinetics during alkene ozonolysis experiments (e.g. Berndt et al.
54 2014a, 2014b, 2015; Newland et al., 2015), and extensive theoretical studies (e.g. Vereecken et al., 2017, and
55 references therein).

56 The reaction of ozone with alkenes proceeds by a concerted addition to the C=C double bond, forming a
57 short lived Primary Ozonide (POZ). Typically, the POZ fragments into two pairs of carbonyls and Criegee
58 intermediates (CI) (Figure 1); for small to medium sized alkenes (C_{≤10}) this POZ is vibrationally excited,
59 decomposing promptly, while for large alkenes (e.g. C_{≥15}, sesquiterpenes), theoretical studies suggest that the POZ
60 can be collisionally stabilized prior to decomposition (Chuong et al., 2004; Nguyen et al., 2009a). Theoretical
61 work also indicates that a small fraction of the POZ can rearrange to a carbonyl-hydroperoxide when vinylic H-
62 atoms are present (Pfeifle et al., 2018); this mechanism is discussed separately below. It has also been suggested
63 that different pathways may play a more significant role for a small number of systems e.g. cyclohexadienes
64 (Pineo et al., 2013).



67 **Figure 1. First step of alkene ozonolysis. A primary ozonide (POZ) is formed which rapidly decomposes to yield a pair**
68 **of chemically activated Criegee intermediates and carbonyl products.**

69 Criegee intermediates are generally zwitterionic in nature, as shown in Figure 1, but the moiety is denoted
70 simply as a >COO structure below (not to be confused with alkylperoxy radicals, ROO*). CI can be formed with
71 the terminal oxygen of the carbonyl oxide moiety in either an *E* (*anti*) or *Z* (*syn*) configuration relative to a given
72 substituent group. The two conformers are not in rapid equilibrium, with quantum calculations showing that the
73 energy barrier to rotational interconversion for CH₃CHOO is about 29 kcal mol⁻¹ (Johnson and Marston, 2008,
74 and references therein); this was confirmed by Vereecken et al. (2017) who calculated barriers exceeding 30 kcal

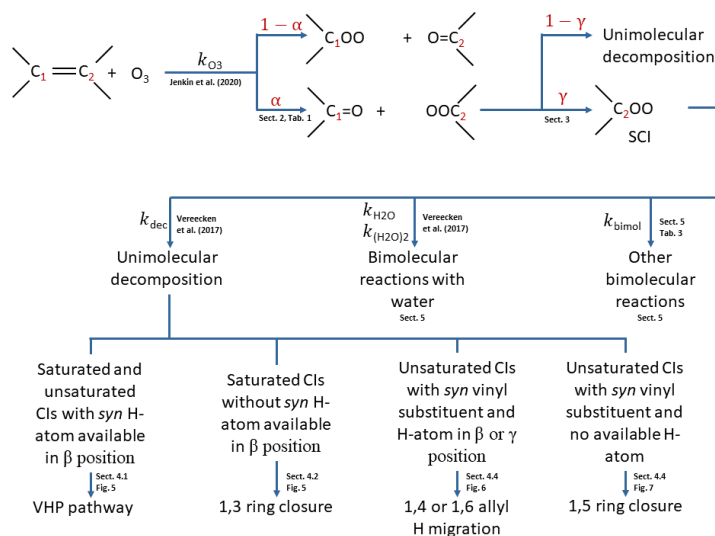


75 mol⁻¹ for saturated CI conformers. Isomeric CI conformers have been shown to have different unimolecular
76 reaction rates (e.g. Vereecken et al., 2017), follow different unimolecular pathways (Herron and Huie, 1977; Niki
77 et al., 1987; Martinez and Herron, 1987; Kidwell et al., 2016), and have very different reaction rates with water
78 (e.g. Taatjes et al., 2013; Sheps et al., 2014; Huang et al., 2015). Therefore, these conformers must necessarily be
79 considered as separate species, irreversibly partitioned according to their nascent ratios, to accurately represent
80 the effects of alkene ozonolysis on atmospheric composition.

81 Structure Activity Relationships (SARs) are commonly used to design the protocols needed to develop
82 automated mechanism generation tools (Vereecken et al., 2018). This paper forms part of a series of articles
83 devoted to the development of SARs for mechanism generation (Jenkin et al., 2018a, 2018b, 2019, 2020). Updated
84 SAR methods for the initial reactions of O₃ with unsaturated organic compounds are presented in a companion
85 paper (Jenkin et al., 2020), while in this work, a protocol is presented for the subsequent chemistry occurring
86 following the initial O₃ addition. This details the yields of carbonyls and Criegee intermediates from the alkene +
87 O₃ reaction, and the subsequent fate of the Criegee intermediates, and accounts for the minor pathway by carbonyl-
88 hydroperoxide radical formation. The protocol is based on available experimental data and theoretical data
89 combined. For areas in which limited data exists, the protocol is set up to be easily updated as new experimental
90 or theoretical results become available. These areas are highlighted in the paper and are recommended areas of
91 further research. The protocol is currently being used to guide development of alkene ozonolysis chemistry in the
92 Generator for Explicit Chemistry and Kinetics of Organics in the Atmosphere, GECKO-A (Aumont et al., 2005),
93 and the Master Chemical Mechanism, MCM (Jenkin et al., 1997, Saunders et al., 2003). It is noted that the protocol
94 does not currently consider aromatic species that have been shown to react with ozone, such as catechols, for
95 which the mechanism may be different to the Criegee mechanism described here.

96 The methodology for applying the protocol described in this work is summarised in Figure 2. The initial
97 addition of ozone to the double bond follows the protocol described in the companion paper (Jenkin et al., 2020).
98 The POZ formed from this protocol then decomposes according to the rules determined in Section 2, to give the
99 primary carbonyl and the CI yields (α), and possibly a minor fraction of carbonyl-hydroperoxide. A fraction (γ)
100 of the CI is then stabilised (Section 3). Both the stabilised and chemically activated CI then follow the relevant
101 set of rules from Vereecken et al. (2017) to ascribe them unimolecular decomposition mechanisms (and hence
102 products) and rates (Section 4), and bimolecular reaction rates with water vapour (Section 5). Finally, bimolecular
103 reaction rates with other atmospherically important species are assigned as a function of the SCI structure (Section
104 5).

105



106

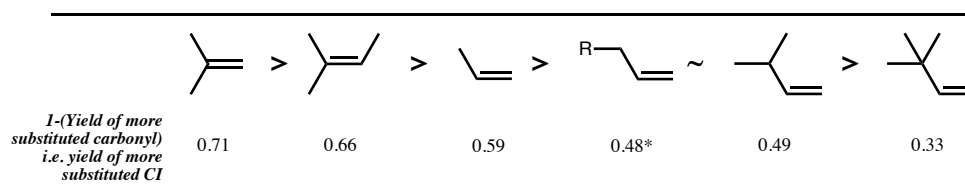
107 **Figure 2. Flow diagram for implementation of the protocol. α = branching ratios in POZ decomposition, γ = fraction**
 108 **of CI stabilised. >COO denotes the Criegee intermediate formed.**

109 2 Primary Ozonide Fragmentation

110 2.1 Alkenes with aliphatic substituents

111 The fragmentation of the POZ has previously been parameterized based on the branching pattern around the
 112 double bond of the parent alkene (Jenkin et al., 1997; Rickard et al., 1999). Generally, it can be said that there is
 113 a preference for formation of the more substituted CI, e.g. the ozonolysis of 2-methyl propene yields ~0.7
 114 $(\text{CH}_3)_2\text{COO}$ and ~0.3 CH_2OO (Rickard et al., 1999). However, consideration of just the immediate substituents
 115 of the double bond breaks down for more complex structures and for oxygenated substituents. There is clearly
 116 also an effect of substitution around the carbon adjacent to the double bond. For instance, when there is a *t*-butyl
 117 group attached to the double bond, a strong preference is seen for formation of the opposing CI, as observed for
 118 yields of trimethylacetaldehyde from 3,3-dimethyl-1-butene (0.67) and *trans*-2,2-dimethyl-3-hexene (0.84)
 119 (Grosjean and Grosjean, 1997). Using data from Grosjean and Grosjean (1997), various homologous series of
 120 alkenes can be considered, such as the series with increasing methyl substitution on the α -carbon. For the 1-alkene
 121 series (Figure 3), yields of the larger carbonyl of 0.35, 0.51, and 0.67 are determined for 1-butene, 3-methyl-1-
 122 butene, 3,3-dimethyl-1-butene respectively.

123



124

125 **Figure 3. Decreasing order of preference, from left to right, of more substituted CI formation from ozonolysis of**
126 **example alkyl substituted alkenes. Values are 1 – (mean of measured yields of carbonyls) (Spreadsheet S1). * Mean**
127 **measured yield of propanal (i.e. 1 – more substituted CI) formation from 1-butene is 0.64, but all other 1-alkenes are**
128 **0.45 – 0.50.**

129 Such relationships have been observed and discussed previously by Grosjean and Grosjean (1997) in terms of: (i)
130 steric hindrance potentially weakening the O-O bond in the POZ on the side of the bulky substituent, and (ii) the
131 inductive effect of adjacent alkyl groups strengthening the O-O bonds in the POZ (Grosjean and Grosjean, 1997).
132 Earlier work considering POZ fragmentation in the aqueous phase (Fliszár and Renard, 1970; Fliszár and Granger,
133 1970; Fliszár et al., 1971) described similar relationships to those observed in the gas phase (i.e. that shown in
134 Figure 3), except in the case of terminal alkenes, for which the reverse trend was observed. In these studies, the
135 observed trends are discussed in terms of stabilisation of the positive charge on the carbon in the POZ through:
136 (i) ‘hyperconjugative stabilisation’ in the transition state, and (ii) the inductive effect during the POZ cleavage,
137 with steric effects discounted as being unimportant in determining the POZ fragmentation pattern.

138 These works can be summarised by saying that it appears that a substituent with a partial negative charge,
139 such as a methyl group, can stabilise the positive charge on the adjacent carbon in the POZ. This leads to a greater
140 yield of the CI containing the more stabilising substituents. On the other hand, a substituent that leads to a partial
141 positive charge on the α -carbon leads to a lower yield of that CI.

142 2.2 Oxygenated alkenes

143 Following the rationale discussed above, oxygenated substituents on the α -carbon might be expected to strongly
144 influence the primary ozonide fragmentation pattern. The number of product yield studies on the ozonolysis of
145 most classes of unsaturated oxygenates is rather limited. As discussed below, some oxygenated substituents appear
146 to destabilise the positive charge on the carbon in the POZ (i.e. disadvantaging POZ fragmentation towards the
147 production of the CI on the oxygenated side), particularly carbonyl groups, while others such as acrylate esters
148 and carboxylic acids may stabilise the CI, favouring its formation. However, data is very limited and often
149 ambiguous for most of the oxygenated classes. This is partly due to challenges in measuring products containing
150 multiple oxygenated groups, partly that some of these classes are likely to be present in negligible amounts in the
151 atmosphere and, for some, that ozonolysis will be a negligible atmospheric sink compared to e.g. reaction with
152 OH or photolysis. The available data is provided in the Supplement, Spreadsheet S1.

153 2.2.1 Enones / enals

154 Primary carbonyl yields have been reported for two α - β terminally unsaturated ketones ($\text{H}_2\text{C}=\text{CHC}(\text{O})\text{R}$). For
155 methyl vinyl ketone (MVK), Grosjean et al. (1993) and Ren et al. (2017) determined a strong preference for
156 formation of the ketone substituted product methyl glyoxal (0.87 and 0.71 ± 0.06 (with no OH scavenger)
157 respectively). For ethyl vinyl ketone, primary carbonyl yields for formaldehyde (HCHO) and 2-oxobutanal have
158 been determined to be 0.55 and 0.44 (Grosjean et al., 1996), and 0.37 and 0.49 (Kalalian et al., 2020) respectively,



159 displaying no clear preference for either fragmentation pathway. For α - β unsaturated ketones ($R_1CH=CHC(O)R_2$),
160 Grosjean and Grosjean (1999) measured the primary carbonyl yields from ozonolysis of 4-hexen-3-one to be:
161 acetaldehyde (CH_3CHO), 0.51 ± 0.01 , and 2-oxobutanal ($CH_3CH_2C(O)CHO$), 0.56 ± 0.02 , while Wang et al. (2015)
162 measured the primary carbonyl yields from ozonolysis of 3-methyl-3-buten-2-one ($CH_2=CR_1C(O)R_2$) to be:
163 diacetyl ($CH_3COCOCH_3$) 0.30 ± 0.03 , and $HCHO$ 0.44 ± 0.05 , and from 3-methyl-3-penten-2-one
164 ($R_1CH=CR_2C(O)R_3$), diacetyl 0.39 ± 0.04 and CH_3CHO 0.61 ± 0.07 . For ozonolysis of 2-enals, yields have been
165 reported for crotonaldehyde (2-butenal) (CH_3CHO 0.42, glyoxal 0.47) (Grosjean and Grosjean, 1997) and trans-
166 2-hexenal (butanal 0.53, glyoxal 0.56) (Grosjean et al., 1996). For the atmospherically important isoprene
167 oxidation product methacrolein (2-methyl-prop-2-enal, MACR), Grosjean et al. (1993) measured yields of methyl
168 glyoxal of 0.58 ± 0.06 and $HCHO$ of 0.12 ± 0.03 . For 2-ethyl acrolein, the ethyl glyoxal yield has been measured to
169 be 0.14 by Grosjean et al. (1994), and 0.49 ± 0.03 by O'Dwyer et al. (2010).

170 To summarise, the presence of a carbonyl group on a double bond appears to favour formation of the
171 opposing CI. However, this effect is neutralised to an extent by the presence of an alkyl substituent on the same
172 side of the double bond, e.g. in the case of 3-methyl-3-buten-2-one, methacrolein, and 2-ethyl acrolein. There
173 remain large uncertainties on the trends in these classes (it is noted that in some cases the sum of the measured
174 primary carbonyl yields is well below one). They clearly warrant further study, owing to the significance of these
175 classes of compounds in atmospheric chemistry (e.g. MACR and MVK from isoprene oxidation (Wennberg et al.,
176 2018)).

177 2.2.2 Enols / enol ethers

178 There has been very little experimental work on the atmospheric chemistry of enols due to difficulties in synthesis,
179 storage, and measurement of these compounds. However, two recent theoretical studies examined the ozonolysis
180 of enols. The first (Lei et al., 2020) on the simplest enol, vinyl alcohol (ethenol), suggested that formation of
181 $CH_2OO + HCOOH$ is strongly favoured ($\sim 78\%$). The second (Wang et al., 2020), on the complex ketene-enol
182 species 4-hydroxy-1,3-butadien-1-one, also suggests that formation of $HCOOH$ and the corresponding CI is
183 strongly favoured (84%). By contrast, there have been several experimental studies on the product yields of the
184 reactions of enol ethers ($R_1-O-CR_2=CR_3R_4$) with ozone. Most studies (Thiault et al., 2002; Klotz et al., 2004;
185 Barnes et al., 2005; Zhou et al., 2006; Zhou, 2007; Al Mulla et al., 2010) have determined that the dominant POZ
186 decomposition channel yields the formate ($R_1-O-C(O)R_2$) and the corresponding CI (R_3R_4COO), with measured
187 yields of the formate ranging from 55% - 89% (see Spreadsheet S1). An exception to these studies is the work
188 of Grosjean and Grosjean (1997; 1999), which tended to find similar yields of the two primary carbonyl products.

189 2.2.3 Esters / acids

190 The primary carbonyl products of ozonolysis of the acrylate esters: methyl acrylate, ethyl acrylate, and methyl
191 methacrylate were studied by Bernard et al. (2010). Grosjean and Grosjean (1997) also studied methyl acrylate.
192 There is no clear evidence for a preferential route for POZ fragmentation in these studies (see Spreadsheet S1).
193 The primary carbonyl yields of vinyl acetate were measured to be 0.30 ± 0.04 and 0.70 ± 0.08 for $HCHO$ and
194 $CH_3C(O)OC(O)H$ respectively by Al Mulla et al. (2010), and 0.20 ± 0.06 and 0.97 ± 0.08 by Picquet-Varrault et al.
195 (2010). These studies suggest a preference for formation of CH_2OO and the acetate. There are only two
196 compounds reported for ozonolysis of α - β unsaturated acids: acrylic and methacrylic acid. For acrylic acid



197 ozonolysis in the presence of formic acid as an SCI scavenger, Al Mulla et al. (2010) measured yields of $1.48 \pm$
198 0.2 and < 0.1 for HCHO and HC(O)C(O)OH respectively, while in the absence of formic acid that group measured
199 a yield of HCHO of 0.95 (Viero, 2008). For methacrylic acid, Al Mulla et al. (2010) measured yields of 0.77 ± 0.07
200 and 0.74 ± 0.10 for HCHO and CH₃C(O)C(O)OH respectively. It is difficult to rationalise these results: the acrylic
201 acid experiments suggest a preference for formation of the CI with the acid moiety, but the methacrylic acid
202 experiments suggest that the presence of a methyl group on the same side of the double bond as the acid reduces
203 this preference, in contrast to most other systems where methyl substitution increases the yield of that CI. This is
204 a recommended area for further study.

205 2.2.4 Alcohols

206 There are significant differences between measured primary carbonyl yields of α,β -unsaturated acyclic alcohols
207 between studies by Grosjean and Grosjean (1997), Le Person et al. (2009), O'Dwyer et al. (2010) and Kalalian et
208 al. (2020). This is likely owing to different experimental setups between groups, and the difficulty of quantitatively
209 measuring compounds with multiple oxygenated substituents. Overall the data in Spreadsheet S1 suggest that the
210 presence of a hydroxyl group in place of a hydrogen on the α -carbon may lead to a slight preference for CI
211 production on the other side of the double bond to the hydroxyl group.

212 2.3 Conjugated alkenes

213 The ozonolysis of conjugated alkenes leads to POZ with a vinyl substituent on the α -carbon. For non-symmetrical
214 conjugated alkenes, the measurement of primary carbonyl yields can only be used to determine the POZ
215 fragmentation if the relative contribution of reaction at each double bond to the overall reaction rate is known. For
216 ozonolysis of the atmospherically important biogenic alkene isoprene, the primary carbonyl yields recommended
217 by IUPAC (Atkinson et al., 2006; iupac-aeris.ipsl.fr, last accessed 6 December 2021) are: methyl vinyl ketone
218 (MVK), 0.17; methacrolein (MACR), 0.41; and HCHO 0.42. Based on reported product yields, the contribution
219 of reaction to each double bond to the overall rate has been estimated to be 0.6 for the terminal double bond and
220 0.4 for the substituted double bond (Nguyen et al., 2016; Jenkin et al., 2020). However, to the authors' knowledge
221 there has been no direct measurement of the reaction at each double bond, and this represents a significant
222 uncertainty in one of the most important atmospheric ozonolysis systems. Based on this assumption, and the
223 recommended yields of MVK and MACR, the formation of MACR+CH₂OO is favoured over methacrolein oxide
224 (MACRO) + HCHO, and there is a slight preference for formation of methyl vinyl ketone oxide (MVKO) +
225 HCHO compared to MVK+CH₂OO. The MACR channel would suggest that the vinyl substituent is destabilising
226 compared to a hydrogen. The methyl group present in MVKO stabilises the CI, leading to a preference for this
227 channel. For symmetrical alkenes, the primary carbonyl yields should be directly representative of the POZ
228 fragmentation. For 1,3-butadiene, an acrolein yield of 51 – 52 % has been measured (Niki et al., 1983; Kramp and
229 Paulson, 2000), suggesting little preference for either POZ decomposition pathway, in contrast to the analogous
230 MACR channel in isoprene. Lewin et al. (2001) reported complementary carbonyl yields from ozonolysis at the
231 internal bond of (*E*) and (*Z*)-penta-1,3-diene and 5-methylhexa-1,3-diene, which all showed a preference for
232 formation of the unsaturated carbonyl (i.e. the saturated CI), suggesting that the vinyl group is less stabilising than
233 a methyl or isopropyl group, in agreement with the observations from isoprene.



234 2.4 Endocyclic alkenes

235 Decomposition of the POZ formed in the ozonolysis of endocyclic alkenes, leads to a molecule containing both
236 the carbonyl oxide and carbonyl moieties. Thus for non-substituted cycloalkenes (e.g. cyclopentene) there is only
237 one possible CI that can be formed (which can be in either the *E* or *Z* configuration). This means that there are no
238 stable primary carbonyls formed and so the relative contributions of the POZ decomposition pathways cannot be
239 inferred from measured primary carbonyl yields as they can for aliphatic compounds. Even a simple endocyclic
240 system such as cyclohexene gives a complex range of gas-phase (Aschmann et al., 2003) and aerosol phase
241 (Kalberer et al., 2000; Ziemann, 2002) products, which can be attributed to decomposition of both the *E* and *Z*
242 forms of hexanal carbonyl oxide. However, the measured OH yields can be used to give an estimate of the amount
243 of CI decomposing via the vinyl-hydroperoxide (VHP) pathway (see section 4.1). It is noted here that it has been
244 proposed that alternative unimolecular pathways (that do not yield OH) are available to the CI formed from
245 endocyclic alkenes (Chuong et al., 2004; Nguyen et al., 2009a; Long et al., 2019), but that these are only dominant
246 for stabilised CI. Since the stabilised CI yield is low for endocyclic alkenes, at least up to C₁₀ (monoterpenes)
247 (Chuong et al., 2004), measured OH yields should give a fair representation of the relative amount of CI
248 decomposing via the VHP pathway). For non-substituted cycloalkenes, OH yields have been compiled by Calvert
249 et al. (2000) covering cyclo-pentene, -hexene, -heptene, -octene and -decene from a number of research groups
250 (Spreadsheet S2). There is some spread in the data but no clear evidence for favouring formation of *E* or *Z* CI, i.e.
251 OH yields tend to centre around ~0.5. For substituted cycloalkenes, Atkinson et al. (1995) measured an OH yield
252 of 0.90 for 1-methyl-1-cyclohexene, suggesting either that the dominant CI formed is the di-substituted CI (which
253 will then undergo decomposition via the VHP pathway to yield OH), or that the mono-substituted CI is formed
254 predominantly as the *syn* conformer. The former must be considered more likely based on the observed trends in
255 aliphatic alkenes for favouring formation of the more substituted CI, and that there appears to be little preference
256 for formation of *syn/anti*-CI from non-substituted endocyclic alkenes. 1-methyl-1-cyclohexene is particularly
257 important from the point of view of atmospheric chemistry as an analogue for the abundant biogenic monoterpenes
258 α -pinene and limonene. OH yields from α -pinene and limonene ozonolysis have been measured by a number of
259 groups and are also generally high (0.64-0.91) (Cox et al. 2020), similar to 1-methyl-1-cyclohexene.

260 2.5 Exocyclic alkenes

261 For exocyclic alkenes in which the double bond is attached to the ring, e.g. β -pinene, the data suggests that POZ
262 fragmentation strongly favours formation of the ring containing CI. For the monoterpene β -pinene, the mean
263 measured yield of the C₉ carbonyl, nopinone, is 0.21 (Grosjean et al., 1993; Hakola et al., 1994; Rickard et al.,
264 1999; Yu et al., 1999; Winterhalter et al., 2000; Hasson et al., 2001b; Lee et al., 2006; Ma and Marston, 2008),
265 with theoretical work (Nguyen et al., 2009b) suggesting that some of this may be secondary and that the primary
266 yield could be even lower. The other two compounds with a terminal double bond attached to the ring for which
267 there are data are camphene (0.36 yield of C₉ carbonyl (Hakola et al., 1994; Hasson et al., 2001b)) and methylene
268 cyclohexane (0.19 yield of C₆ carbonyl (Hasson et al., 2001b)). For the monoterpene sabinene, which has a
269 terminal double bond attached to a C₅ and C₇ ring, the mean measured yield of the C₉ carbonyl, sabinaketone, is
270 0.44. This is considerably higher than from those compounds where the double bond is on a C₆ ring, probably
271 demonstrating the impact of ring strain on the POZ fragmentation. The monoterpene terpinolene has a
272 disubstituted double bond attached to a six membered ring. Reported yields of the ring containing carbonyl



273 (0.40±0.06 (Hakola et al., 1994); 0.40±0.08 (Reissell et al., 1999); 0.45 (Ma and Marston, 2009)) suggest yields
274 of the ring containing CI of 0.60 and 0.55 respectively; this assumes 100% reaction at the exocyclic double bond,
275 with Hakola et al. (1994) measuring a yield of $\leq 2\%$ of the dicarbonyl expected as a product (though by no means
276 the only one) from reaction at the endocyclic double bond. These CI yields are lower than for the exocyclic alkenes
277 with terminal double bonds, but are still considerably higher than most compounds which have a dimethyl
278 substitution on the double bond, for which acetone yields tend to be ~ 0.3 . The presence of a ring clearly has a
279 different effect to simply having two alkyl groups attached to the double bond, leading to much higher yields of
280 the ring containing CI.

281 For alkenes with a vinyl group attached to a ring, there are data only for vinyl cyclohexane, and its aromatic
282 analogue styrene. These have similar yields for the ring containing carbonyl of 0.62 and 0.64 respectively
283 (Grosjean and Grosjean, 1997). There is no data for alkenes with double bonds more distant from a ring.

284 2.6 Yields of CI stereo-conformers

285 The formation of *syn/anti* conformers of CI in alkene ozonolysis was first discussed by Bauld et al. (1968), to
286 explain the observed *cis/trans* yields of the secondary ozonide formed from ozonolysis in the aqueous phase. Their
287 observations suggested that ozonolysis of *cis*-alkenes will predominantly form *anti*-CI, while for *trans*-alkenes
288 the predominance was less clear and appeared to be dependent on alkene structure. In the gas phase, but-2-ene is
289 the most studied system. Various experimental work has observed higher yields of OH from *trans*-but-2-ene
290 compared to *cis*-but-2-ene (see Spreadsheet S3). Assuming that only (*Z*)-CI decomposition yields OH (see Section
291 4.1), this implies a higher nascent (*Z*):(*E*)-CH₃CHO ratio from decomposition of the POZ formed in *trans*-but-
292 2-ene ozonolysis. Orzechowska and Paulson (2002) measured a ratio of 1.62 for the OH yields from *trans/cis*-
293 but-2-ene. They observed a similar relationship for *trans/cis*-pent-2-ene and *trans/cis*-hex-3-ene, with OH yield
294 ratios determined as 1.80 and 1.51 respectively. Assuming that OH comes exclusively from (*Z*)-CH₃CHO
295 implies a (*Z*):(*E*)-RCHO ratio of 0.60:0.40 – 0.64:0.36 for these three systems. Kroll et al. (2002) determined a
296 similar OH yield ratio for *trans/cis*-hex-3-ene, but using isotopically labelled hydrogen atoms demonstrated that
297 a fraction of this OH was not coming from the (*Z*)-CI. From their OH yield measurements, they inferred a (*Z*):(*E*)-
298 C₂H₅CHO ratio of 50:50 for *trans*-3-hexene, and 20:80 for *cis*-3-hexene. Campos-Piñeda (2017) reported direct
299 measurements of the vinoxy radical formed in decomposition of *syn*-CH₃CHO, from *cis*- and *trans*-but-2-ene
300 ozonolysis, inferring a yield of *syn*-CH₃CHO of ~ 0.5 from *trans*-but-2-ene and ~ 0.3 from *cis*-but-2-ene, broadly
301 in line with estimations from measured OH yields.

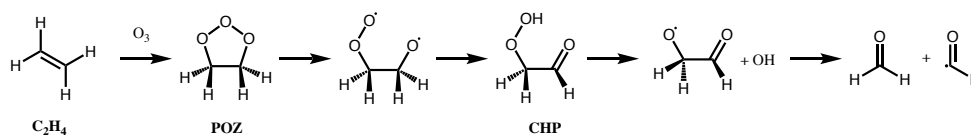
302 Early theoretical calculations considering the gas phase (Cremer, 1981a,b) suggested that (*Z*)-RCHO is
303 likely to be formed in greater yield for small alkenes, but that (*E*)-RCHO becomes more favoured in the
304 ozonolysis of large alkenes. Calculations by Rathman et al. (1999) suggested that (*Z*)-CH₃CHO should be
305 favoured in *trans*-but-2-ene ozonolysis, but that conversely (*E*)-CH₃CHO would be favoured in *cis*-but-2-ene
306 ozonolysis. Recent theoretical work (Watson, 2021) looking at POZ fragmentation for a series of disubstituted 2-
307 alkenes (CH₃CH=CHR), suggests formation of (*E*)-RCHO will be strongly favoured in the ozonolysis of *cis*-
308 alkenes (87 % for *cis*-but-2-ene, increasing to 93 % for *cis*-2-hexene), while there is a roughly equal split from
309 ozonolysis of *trans*-alkenes. This is in qualitative agreement with the experimental work discussed above but
310 suggests a stronger preference than observed in the direct measurements of the vinoxy radical by Campos-Pineda
311 (2017). For tri-substituted alkenes, Watson (2021) finds a strong preference for formation of (*E*)-RCHO on the



312 mono-substituted side of the double bond. For the C₄-CI formed in isoprene ozonolysis, theoretical calculations
313 have determined a relative split of 50:50 for the two conformers of MVKO (Kuwata et al., 2005), and 20:80 for
314 *syn*-MACRO:*anti*-MACRO (Kuwata and Valin, 2008). This is in qualitative agreement with the observed low
315 OH yield (0.08-0.13) from 1,3-butadiene (Atkinson and Aschmann, 1993; Kramp and Paulson, 2000) if it is
316 assumed that decomposition of *syn*-MACRO will have a high OH yield whereas *anti*-MACRO will not yield OH.
317 To the authors' knowledge there is no other information on the relative yields of *syn/anti*-R₁R₂COO (where R₁ ≠
318 R₂).

319 2.7 POZ ring opening to a biradical

320 In addition to direct CI + carbonyl formation from the POZ, the possibility exists of ring opening of the POZ to a
321 singlet alkoxy-peroxy biradical (>C(O')-C(OO')<) (O'Neal and Blumstein, 1973; Olzmann et al., 1997; Anglada
322 et al., 1999; Fenske et al., 2000; Nguyen et al., 2015; Pfeifle et al., 2018) (Figure 4). In addition to re-closing the
323 ring to the POZ or decomposing to CI + carbonyl, this alkoxy-peroxy biradical can migrate an H-atom from the
324 alkoxy-bearing carbon, forming a carbonyl hydroperoxide (-C(=O)-C(OOH)<); this pathway is only possible if
325 the alkene has a vinylic H-atom. The carbonyl hydroperoxide formed has a high energy content, over 100 kcal
326 mol⁻¹, and can eliminate an OH radical, forming a α -carbonyl-alkoxy radical that rapidly decomposes to an acyl
327 radical and a carbonyl. This pathway has been invoked in theoretical studies as the main source of OH in the
328 ozonolysis of ethene (in which OH cannot be formed via a VHP) (Nguyen et al., 2015; Pfeifle et al., 2018), and
329 is expected to contribute somewhat to OH formation in other alkenes, though this has not yet been investigated
330 experimentally or theoretically. Alternative proposed sources of OH in ethene ozonolysis all involve the CH₂OO
331 Criegee intermediate. However, theory has shown that direct OH formation from CH₂OO by a 1,3-H-migration
332 involves too high a barrier (e.g. Nguyen et al., 2015; Pfeifle et al., 2018), while OH elimination from the hot
333 formic acid formed in the 1,3-ring closure (see Section 4.2) is not competitive against formation of H₂O + CO and
334 H₂ + CO₂, as also borne out by HCOOH pyrolysis experiments (Chang et al., 2007; Vichiatti et al., 2017). The
335 carbonyl hydroperoxide route thus resolves an apparent discrepancy between ethene ozonolysis experiments,
336 which observe significant OH yields, and experiments (Stone et al., 2018) and theoretical work (Nguyen et al.,
337 2015; Pfeifle et al. 2018), which indicate very little OH formation from CH₂OO. Pfeifle et al. (2018) calculated a
338 yield of 12.3 % for the carbonyl-hydroperoxide in ethene ozonolysis, while Nguyen et al. (2015) obtained 13 %,
339 both at the low end of the current IUPAC recommended OH yield (0.17±0.05) for the reaction (Cox et al., 2020).
340



342 Figure 4. The carbonyl hydroperoxide (CHP) decomposition pathway for ethene ozonolysis

343



344 2.8 Protocol Rules for POZ fragmentation

345 2.8.1 POZ fragmentation

346 A group contribution approach was designed to estimate POZ fragmentation yields. The approach assumes that
347 the branching ratio for the two possible fragmentations of the POZ depends on the substituents of the
348 $R_{1a}(R_{1b})C=C(R_{2b})R_{2a}$ parent alkene. The general form of the relationship is given by:
349

$$350 Y_{CI1} = \frac{(F_{1a}+F_{1b})-(F_{2a}+F_{2b})+1}{2} = 1 - Y_{CI2} \quad (E1)$$

351 where Y_{CI} is the CI production yield on the i^{th} carbon and F_R are the contributions for the 4 substituents on the
352 C=C bond. The set of F_R values is developed based on the observed primary carbonyl yields (Supplementary
353 Section S1 and Spreadsheet S1) and are based on a least squares fit to a relevant dataset of alkenes for each
354 substituent (Figures S1-S5).

355 For a vinyl group, F is constrained to fit the IUPAC recommended yields of MVK and MACR from
356 isoprene ozonolysis, assuming that ozone reacts 60% at the terminal double bond and 40% at the substituted
357 double bond (Nguyen et al., 2016; Jenkin et al., 2020). The presence of a carbonyl group adjacent to the double
358 bond appears to strongly favour formation of the opposing CI in the case of MVK (i.e. -C(=O)H). However, this
359 is not the case for alkenes with the structure -C(=O)R in the database, for which there appears to be no clear
360 preference for formation of either CI, with a fit to the data yielding a slightly positive F value of 0.127. The
361 strongest negative effect (i.e. leading to formation of the carbonyl containing the functional group) observed in
362 the database is for enol ethers (-OR), giving an F value of -0.655. This is assumed to also be the same case for
363 enols (-OH) based on the theoretical calculations of Lei et al. (2020) and Wang et al. (2020), and for vinyl esters
364 (-OC(=O)R), based on the observed values for vinyl acetate. By contrast, an acrylate ester (-C(=O)-O-) substituent
365 adjacent to the double bond does not appear to have a strong effect on fragmentation, and $F = 0$ is used. Similarly,
366 the trend from the two unsaturated acids reported is unclear, and $F = 0$ is also used here. An OH group on the
367 alpha carbon appears to slightly decrease Y_{CI} compared to an H atom, but the data is currently too limited to
368 recommend a group additivity value, so the OH group is treated as an H atom, i.e. $F_{-CH_2OH} = F_{-CH_3}$. More distant
369 oxygenated groups are not considered. The available data for exocyclic alkenes with the double bond attached to
370 the ring is not able to take into account the effect of multiple rings, with F_{ring} being determined from only
371 exocyclic alkenes with C_6 rings (β -pinene, methylene cyclohexane, and terpinolene). For rings with a vinyl group
372 attached, $F_{(C_6)\text{ring}}$ is determined only from C_6 rings, i.e. styrene and vinylcyclohexane. Endocyclic alkenes are
373 assumed to follow the same fragmentation patterns as acyclic alkenes. For example, cyclohexene is considered to
374 have the structure $>CH_2CH_2CH=CHCH_2CH_2<$, 1-methyl cyclohexene $>CH_2CH_2C(CH_3)=CHCH_2CH_2<$ etc.

375 The group contribution value, F , is then used in Eq. (1) to determine the yield of CI_1 (defined as having
376 substituents 1a and 1b) from the general structure $R_{1a}(R_{1b})C=C(R_{2b})R_{2a}$. Generally, the measurement of the larger
377 primary carbonyl was used to determine the primary carbonyl and CI yields. This is because in some cases, the
378 smaller carbonyl can be formed as a decomposition product of the larger CI and hence is not a true primary
379 carbonyl yield.

380



381
382

Table 1. Group contribution values (*F*) for various substituents

Group	Value	Alkenes used for fit
=ring	+ 0.62	β -pinene, methylene cyclohexane, terpinolene
-CH ₃	+ 0.218	propene, 2-methyl butene, 2-methyl-but-2-ene
-C(=O)R	+ 0.127	2-ethylacrolein, ethyl vinyl ketone, 4-hexen-3-one, 3-methyl-3-buten-2-one, 3-methyl-3-penten-2-one, 2-butenal, trans-2-hexenal
-CH ₂ CH ₃	+ 0.107	but-1-ene, 2-methyl-but-1-ene, 2-ethyl-but-1-ene, 2,2-dimethyl-hex-2-ene
-H	0	By definition
-COOH, -C(=O)-O-R,	0	Acids and acrylate esters, see spreadsheet S1
-CH ₂ CH ₂ R	0	pent-1-ene, hex-1-ene, hept-1-ene, oct-1-ene, dec-1-ene, 2-methyl-pent-1-ene
-CHR ₁ R ₂	- 0.069	3-methyl-but-1-ene, 3-methyl-pent-1-ene, 2,3-dimethyl-but-1-ene, 2,4-dimethyl-pent-2-ene, 2,3,4-trimethyl-pent-2-ene, 3-methyl-2-isopropyl-but-1-ene
-(C ₆)ring	- 0.25	styrene, vinyl cyclohexane
-vinyl	- 0.28	isoprene
-CR ₁ R ₂ R ₃	- 0.386	2,3,3-trimethyl-but-1-ene, 2,4,4-trimethyl-pent-2-ene, 2,2-dimethyl-hex-3-ene, 3,3-dimethyl-but-1-ene
-OR, -OH, -(OC(=O)R)	- 0.655	methyl vinyl ether, ethyl vinyl ether, propyl vinyl ether, butyl vinyl ether, ethyl propenyl ether

383 2.8.2 *E/Z* conformer yields

384 In light of the current paucity of experimental and/or theoretical information on the relative yields, an equal 0.5:0.5
385 yield is assigned as a default value for (*E*)/(*Z*) isomers for all asymmetrical CI. The following two exceptions are
386 nevertheless considered. For acyclic *cis*-RCH=CHR parent alkenes, a relative yield of 0.7:0.3 is set for (*E*):(*Z*) CI.
387 For conjugated structures, formation of (*E*)/(*Z*)->C=C(R)-CHOO is assumed to be in a ratio of 0.8:0.2, based on
388 the work of Kuwata et al. (2005) and Kuwata and Valin (2008).

389 2.8.3 Carbonyl-hydroperoxide route

390 While there is little information available on the stepwise carbonyl-hydroperoxide POZ decomposition
391 mechanism, it is needed to account for the radical yields observed in the ozonolysis of ethene as discussed above.
392 There is no reason to assume it will not occur more generally for any alkenes with vinylic H-atom(s), though
393 perhaps with different fates of the intermediate biradical or carbonyl hydroperoxide. Currently this channel is only
394 included for the ethene-ozone reaction, for which it is assumed that 0.12 of the ethene-ozone reaction forms the
395 biradical intermediate, rather than the CI + carbonyl, using the contribution calculated for the carbonyl
396 hydroperoxide channel by Pfeifle et al. (2018). When more general data become available, assuming the channel
397 is active for other systems, the protocol will be updated. The general structure of such a scheme might be: the
398 POZ is assumed to break either of the O-O bonds with equal probability, forming one of two possible biradicals.
399 If there is an available vinyl α -hydrogen, it is assumed that the H-shift to the peroxy radical occurs, forming the
400 carbonyl-hydroperoxide (R₁R₂C(OOH)C(=O)R₃), followed by loss of OH and scission of the C-C bond to yield
401 the stable product R₁R₂C=O and the radical R₃C=O. If there is no available α -hydrogen, the biradical is assumed
402 to yield the CI and carbonyl, either by C-C fragmentation or recyclisation to the POZ.

403 3 Stabilisation of the Criegee Intermediate

404 3.1 Excited vs. stabilised CI

405 Following decomposition of the primary ozonide, CI are formed with a broad range of internal energies (e.g.
406 Drozd et al., 2011). Consequently, it is often useful to consider the mean energy of a population of CI. Those



407 generated with a high internal energy, allowing prompt chemical reactions, are called excited, or chemically
408 activated CI (CI*). Those without enough internal energy to undergo prompt decomposition are considered to be
409 ‘stabilised’ CI (SCI). Additionally, CI* can be collisionally stabilised. This has been demonstrated by
410 experimental work showing that SCI yields are pressure dependent (Drozd et al., 2011, Hakala and Donahue,
411 2016; 2018). Note that this pressure dependence is moderate, and across the range of relevant atmospheric
412 pressures not of primary concern; we base our analysis on the available data near 1 atm.

413 3.2 SCI Yield

414 The total SCI yield for a given alkene is the sum of the fraction of the nascent CI population that is formed
415 stabilised, plus the fraction of CI* that is collisionally stabilised. The fate of the CI* is a competition between
416 prompt unimolecular decay and collisional stabilisation, with the CI* having a lifetime on the order of
417 nanoseconds against either of these processes (e.g. Drozd et al., 2017; Stephenson and Lester, 2020). Most alkenes
418 will form a number of different CI*, each with different lifetimes against unimolecular decay and collisional
419 stabilisation. The rate of collisional stabilisation of a given CI* is dependent on the frequency of collisions (and
420 hence pressure), and the efficiency of energy loss to the bath gas. The rate of unimolecular decay of a given CI*
421 depends on: (i) the energy of the CI* when formed, (ii) the activation energy for the most facile decay process /
422 the energy required for tunnelling, and (iii) the relative density of states of the reactants and transition state, i.e.
423 the entropy of the reaction. The dominant unimolecular decay mechanism is dependent on the structure of the CI;
424 these mechanisms are discussed in Section 5.

425 Larger CI* will tend to be stabilised to a greater extent due to a greater density of states distributing the
426 excess internal energy over a greater number of modes and so reducing the rate of unimolecular decay (Drozd and
427 Donahue, 2011; Stephenson and Lester, 2020). However, as the size of the CI increases relative to the carbonyl
428 co-product formed in POZ decomposition, the fraction of the energy taken by the CI from the POZ will increase
429 (assuming the energy has time to become equally distributed throughout the CI), decreasing the mean energy of
430 the nascent CI population and hence the fraction of CI* with enough energy to undergo unimolecular decay
431 (Fenske et al., 2000; Newland et al., 2020). This will lead to greater stabilisation. For endocyclic alkenes,
432 decomposition of the POZ produces a single molecule containing both the carbonyl and carbonyl oxide moieties.
433 Such CI have a high initial energy, with no energy lost from the POZ decomposition to relative motion of the
434 fragments, and thus require many collisions to be quenched (Vereecken and Francisco, 2012). Consequently,
435 endocyclic alkenes with $\leq C_7$ have little stabilisation (Hatakeyama et al., 1984; Campos-Pineda and Zhang, 2017;
436 Drozd and Donahue, 2011). For the endocyclic C_{10} monoterpenes α -pinene and limonene, total SCI yields have
437 been measured to be 0.13-0.22 (Hatakeyama et al., 1984; Taipale et al., 2014; Sipilä et al., 2014; Newland et al.,
438 2018) and 0.23-0.27 (Sipilä et al., 2014; Newland et al., 2018) respectively. For the C_{15} sesquiterpene β -
439 caryophyllene, a total SCI yield (including from decomposition of the stabilised POZ) of 0.74 was calculated by
440 Nguyen et al. (2009), with a value of > 0.6 determined experimentally (Winterhalter et al., 2009).

441 Total SCI yields have been measured experimentally for many alkene-ozone systems. These are generally
442 determined indirectly, by performing ozonolysis experiments in the presence of an SCI scavenging species (e.g.
443 H_2O , SO_2 , hexafluoroacetone). Measurements of scavenger removal, or formation of products from the SCI +
444 scavenger reaction, are used to determine the SCI yield. Yields measured in such a way must be considered to be
445 lower limits since, under most experimental conditions, a significant fraction of the SCI may undergo



446 unimolecular decomposition based on recently reported fast SCI decomposition rates (e.g. Newland et al., 2015;
447 Vereecken et al., 2017; Newland et al., 2018). The choice of scavenger species is also important. In some older
448 experimental studies, water was used as an SCI scavenger, with H₂O₂ (e.g. Hasson et al., 2001a) or hydroxymethyl
449 hydroperoxide (HMHP, e.g. Hasson et al., 2001a; Neeb et al., 1997) being the detected reaction products. For
450 mono-substituted (*E*)-SCI, or for CH₂OO, this may be a reasonable assumption, with $k_{(H_2O+SCI)}[H_2O]/k_{(decomp.)} \sim$
451 $10^2 - 10^3$ at $[H_2O] = 5 \times 10^{17} \text{ cm}^{-3}$ (e.g. Vereecken et al., 2017). However, for (*Z*)-SCI, $k_{(H_2O+SCI)}[H_2O]/k_{(decomp.)} \sim$
452 $10^2 - 10^1$, i.e. the majority of the SCI will not be scavenged by H₂O.

453 3.3 Protocol Rules for CI Stabilisation

454 The relationship between stabilisation of the CI* and size of the carbonyl co-product has been studied for CH₂OO
455 and (CH₃)₂COO by Newland et al. (2020) (Figure 5). For CH₂OO this relationship might be expected to represent
456 a minimum for CI* that primarily decay via the 1,3 ring closure pathway (i.e. *anti*-CI*, see Section 4.2), since
457 larger CI* will have a slower decay rate due to a greater density of states. Similarly, the trend for (CH₃)₂COO can
458 be assumed to be close to a minimum for CI* that primarily undergo the 1,4 vinylhydroperoxide (VHP)
459 decomposition pathway (see Section 4.1), with only *syn*-CH₃CHOO likely to have a lower density of states (and
460 therefore faster decomposition) (Stephenson and Lester, 2020). With no further data available, the stabilisation
461 trend of CH₂OO is used for CI* that decompose via 1,3 ring closure, while that of (CH₃)₂COO is used for CI* that
462 decay via the 1,4 vinylhydroperoxide pathway. For other pathways, such as the 1,5-ring closure to a dioxole (see
463 Section 4.4), important in isoprene ozonolysis, no information is available. CI* with a vinyl group *syn* to the
464 terminal oxygen of the carbonyl oxide are considered as *syn*-CI for the purposes of calculating stabilisation in the
465 protocol.

466 An extension of Equation E7 in Newland et al. (2020) is used to estimate the CI stabilisation *S*:

467

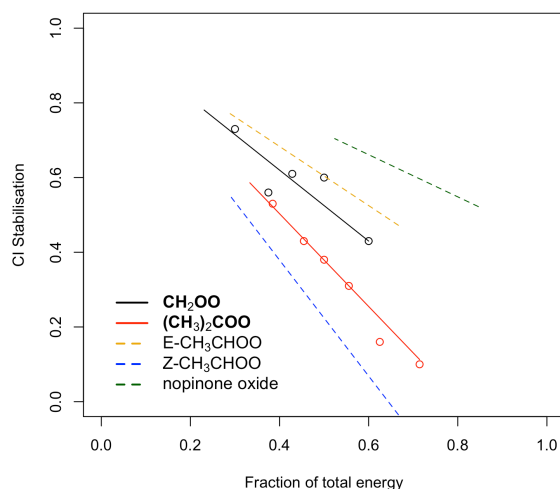
$$468 \quad S = 1 - \left[\left(\frac{A_{CI}}{A_{tot}} \right) \times F \times z_{path} \right] \quad (E2)$$

469 where *A_{CI}* is the total number of non-hydrogen atoms in the CI*, *A_{tot}* is the total number of non-hydrogen atoms in
470 the POZ, and *F_{VHP}* and *F_{13RC}* are values determined for CH₂OO and (CH₃)₂COO based on the SCI yields for their
471 symmetrical parent alkenes ethene and 2,3-dimethylbut-2-ene, respectively. For CH₂OO this is 0.95 and for
472 (CH₃)₂COO it is 1.24 (Newland et al., 2020). In this work, an additional term, *z_{path}*, is included to take into account
473 the observed / predicted increased stabilisation of CI* with size. For CI* that decay via the 1,3 ring closure
474 pathway, *z_{13RC}* is defined as $x / (A_{CI} + (x - A_{CH_2OO}))$, where *A_{CH₂OO}* is the total number of non-hydrogen atoms in
475 CH₂OO (i.e. 3), and *x* is an adjustable parameter. For CI* that decay via the 1,4 H-shift, *z_{VHP}* is defined as $x / (A_{CI}$
476 $+ (x - A_{(CH_3)_2COO}))$, where *A_{(CH₃)₂COO}* = 5. In both terms, *x* = 5, and has been optimized to improve the fit between
477 measured and calculated total SCI yields of larger alkenes (Newland et al., 2020).

478 Figure 5 shows the measured CI* stabilisation for CH₂OO and (CH₃)₂COO as a function of the total
479 energy taken from the POZ by the CI*, from Newland et al. (2020). Fits to the measured data are calculated using
480 Eq. (2). Also shown are the calculated stabilisation trends for (*E*)- and (*Z*)-CH₃CHOO and nopinone oxide (the C₉
481 CI* formed in β-pinene ozonolysis). Figure 5 shows that stabilisation of *E*-CI* is predicted to be considerably
482 greater than for *Z*-CI* when formed with the same energy. For CH₃CHOO it is noted that very little (0.11)
483 stabilisation of (*Z*)-CH₃CHOO* is predicted when produced from but-2-ene ozonolysis (fraction of total energy



484 = $A_{CI}/A_{tot} = 4/7 = 0.57$), whereas a much greater stabilisation of (*E*)-CH₃CHOO* is predicted. Using the *E/Z*-
485 RCHOO yields given in Section 2.8.2 for *cis* and *trans* alkenes, and the trends presented in Figure 5, then a total
486 SCI yield of 0.33 for *trans*-but-2-ene and 0.42 for *cis*-but-2-ene is calculated, in good qualitative agreement with
487 the relationship observed in Newland et al. (2015). The calculated values for nopinone oxide demonstrate the
488 decreasing sensitivity of CI* stabilisation to the co-product size as the size of the CI* increases.



489

490 **Figure 5. Dependence of CI* stabilisation on the fraction of the total energy taken from the POZ. Black (CH₂OO) and**
491 **red ((CH₃)₂COO) points, measurements taken from Newland et al. (2020). Solid and dashed lines, fits calculated using**
492 **Eq. (2).**

493 For endocyclic alkenes, an empirically derived sigmoid fit (Supplementary Section S2: Equation S1; Figure
494 S6) is applied to the very limited dataset that shows $Y_{SCI} \approx 0$ for $C \leq 7$, $Y_{SCI} \approx 0.2$ for monoterpenes, and $Y_{SCI} \approx$
495 0.74 for sesquiterpenes.

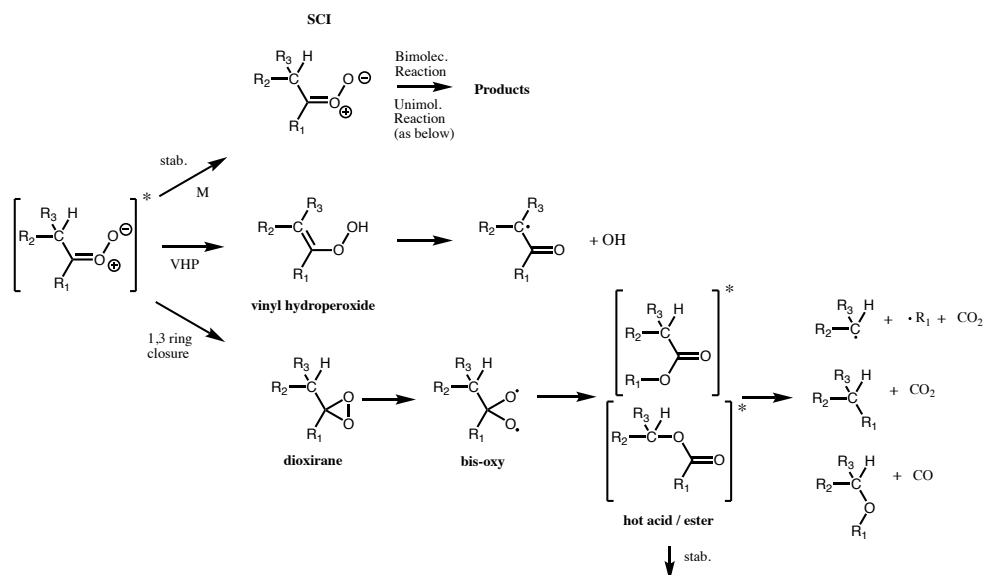
496 4 Unimolecular reactions of CI* and SCI

497 CI can undergo unimolecular isomerisation / decomposition. The unimolecular pathways available to SCI are
498 assumed to be the same as those available to CI* (although it is noted that there is little evidence to back up this
499 assumption). However, while for CI* these processes are prompt, occurring on a timescale of 10^{-9} s (Drozd et al.,
500 2017), for SCI they occur at a range of rates such that their competition with atmospheric bimolecular reactions
501 needs to be considered. A wide range of unimolecular isomerisation / decomposition pathways have been
502 characterised for CI, but only two of these are believed to be important for saturated CI under atmospheric
503 boundary layer conditions (Vereecken et al., 2017): a 1,4 H-migration, i.e. the vinylhydroperoxide pathway, and
504 a 1,3 ring closure, i.e. the hot acid / ester pathway (Figure 6). If the vinylhydroperoxide pathway is available, then
505 this will always be the dominant decomposition pathway as it is the energetically most facile, with only a slight
506 entropic disadvantage compared to the 1,3 ring closure (Vereecken et al., 2017). Unsaturated CI have some
507 additional pathways available (see Section 4.4).

508 Experimentally determined decomposition rates are available only for a limited number of SCI. Early
509 estimates were considerably slower than more recent experimental evidence. Vereecken et al. (2017) recently



510 published an extensive SAR providing temperature dependent unimolecular rates and mechanisms for a wide
511 range of SCI structures based on theoretical calculations tied to experimental work as well as group additivity
512 relations.



513

514 **Figure 6.** Available pathways for a CI with a hydrogen atom available in beta position to the carbonyl oxide. From top
515 to bottom, the available pathways are the stabilisation (stab.) pathway, the vinylhydroperoxide (VHP) pathway and
516 the 1,3 ring closure (hot acid/ester) pathway.

517 4.1 Vinylhydroperoxide (VHP) pathway

518 A CI with a β -hydrogen atom in a *syn* orientation to the terminal oxygen atom of the carbonyl oxide can isomerise
519 to form a vinylhydroperoxide via a 5-membered transition cycle (Figure 6). This route is therefore available to
520 monosubstituted (*Z*)-CIs and disubstituted CIs. The VHP formed has a short lifetime and promptly or thermally
521 decomposes to form an OH radical and a β -acylalkyl (vinoxy) radical, in some cases with a small yield of β -acyl-
522 alcohols (Taatjes et al., 2016; Kuwata et al., 2018). The OH radicals are thus formed on a short time scale (e.g.
523 Drozd et al., 2017) directly from the VHP decomposition. The β -acylalkyl radical reacts with O_2 to form a β -
524 acylperoxy radical. On a longer timescale, the subsequent chemistry of this peroxy radical can yield further HO_2
525 and OH radicals (e.g. Nguyen et al., 2016).

526 The best studied system that follows the 1,4 H-shift pathway is stabilised $(CH_3)_2COO$. Experimentally
527 derived rates are fast ($300 - 1000 s^{-1}$) (Berndt et al., 2014b; Newland et al., 2015; Chhantyal-Pun et al., 2016;
528 Smith et al., 2016). The experimental evidence also shows a strong temperature dependence, with measured rates
529 varying from $269 s^{-1}$ at 283 K to $916 s^{-1}$ at 323 K (Smith et al., 2016). This is in good agreement with the SAR of
530 Vereecken et al. (2017) which shows that the rate of decomposition of saturated SCI is fastest (ca. $500 s^{-1}$) for
531 those SCI with access to the VHP route. This SAR shows that the rate is slowed by more than an order of
532 magnitude when only one H atom is available on the α -carbon and that the rates are also affected by the *anti*
533 substituent, with the presence of a vinyl group reducing rates by an order of magnitude, and the presence of a
534 carbonyl group reducing rates by two orders of magnitude.

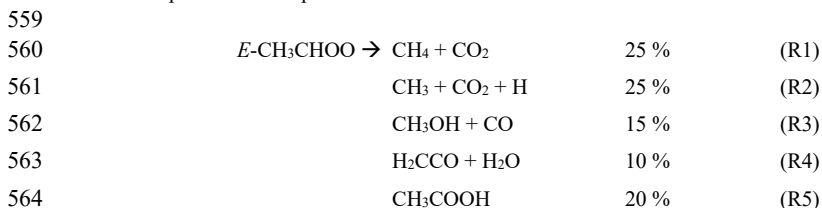


535 This pathway may not be available to certain CI structures even though there is an available hydrogen on
536 the α -carbon. This is the case for the bicyclic C_9 CI formed in ozonolysis of the monoterpene β -pinene, with the
537 terminal oxygen facing the four membered ring. Calculations have shown that formation of the vinyl
538 hydroperoxide is not possible for this CI due to the strain it would put on the ring, and so the dominant
539 decomposition pathway is 1,3 ring closure (Nguyen et al., 2009b). This has also been shown to be the case for the
540 cyclic C_9 CI formed facing the three membered ring in the ozonolysis of sabinene (Almatarneh et al., 2019).

541 4.2 1,3 ring closure

542 For monosubstituted (*E*)-CI and CH_2OO (see Section 5.3), decomposition via a VHP is not available. Instead
543 unimolecular reaction proceeds predominantly via a 1,3 ring closure, with typical rates $\leq 10^2 \text{ s}^{-1}$ (Vereecken et al.
544 2017), to a chemically activated dioxirane species (Figure 6). This breaks the weak O-O bond giving a singlet bis-
545 oxy radical (Wadt and Goddard, 1975; Herron and Huie, 1977; 1978). Various pathways have been proposed for
546 the subsequent chemistry of this species based on observed product distributions (Chen et al., 2002). This pathway
547 has been characterised best for CH_2OO (Section 5.3). The dioxirane is thought to rearrange to a ‘hot’ acid / ester,
548 which can undergo decomposition to yield a range of products. As the size of the CI increases, the hot acid / ester
549 is predicted to be more likely to be collisionally stabilised (Vereecken and Francisco, 2012).

550 There have been very few experimental studies to date on the products of isomerisation / decomposition
551 of (*E*)-RCHOO. This is challenging experimentally as (*E*)-RCHOO will always be formed as a partner with (*Z*)-
552 RCHOO. The most studied (*E*)-CI is (*E*)- CH_3CHOO , with observed products from *cis/trans*-but-2-ene ozonolysis
553 (which yields (*E*)- and (*Z*)- CH_3CHOO as the CI products) of HCHO, CH_3COOH , CH_3OH , CH_4 , CHOCHO,
554 ketene, CO and CO_2 (e.g. Tuazon et al., 1997; Grosjean et al., 1994). With the exception of glyoxal, these can all
555 be rationalised as decomposition products of ‘hot’ (*E*)- CH_3CHOO via various pathways (Reactions R1 – R5). The
556 relative proportion of each channel is based on the reported yields in Tuazon et al. (1997), except for CH_3COOH ,
557 from Grosjean et al. (1994), although it is noted that CH_3COOH may be a product of CH_3CHOO + water vapour
558 in their experimental setup.



566 For R_1R_2COO decomposition via 1,3 ring closure, products are formed via a ‘hot’ ester. There has been very little
567 work on the relative contribution of decomposition channels and stabilisation for these species. For example, there
568 is no experimental work to validate the predicted trend of increasing stabilisation of the hot acid / ester with size,
569 or at what size this becomes important. For the large terpenoid compounds β -pinene (Nguyen et al., 2009b) and
570 β -caryophyllene (Nguyen et al., 2009a), the acids/lactones formed from isomerisation of the C_9 -dioxirane have
571 been predicted to be fully stabilised.

572
573



574 **4.3 CH₂OO**

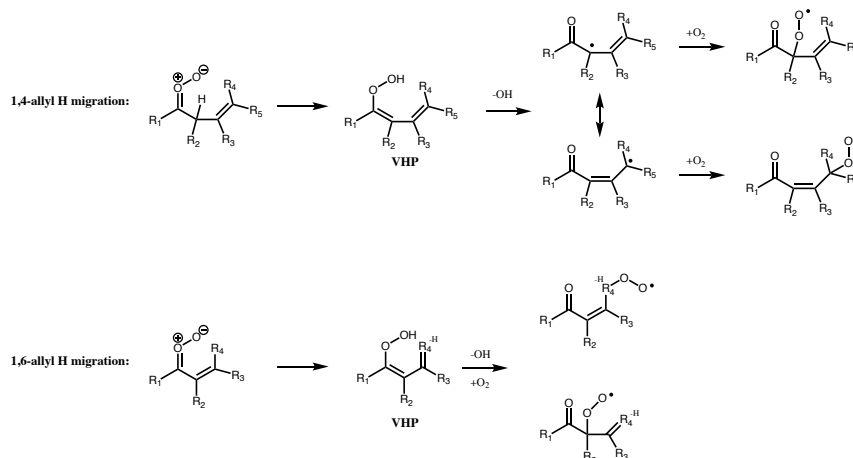
575 CH₂OO also follows the 1,3-ring closure pathway but is considered separately here as it has been the subject of a
576 considerable body of work. Experimentally reported products from CH₂OO decomposition include: CO₂, CO, H₂,
577 OH, HO₂, H₂O, and HCOOH (e.g. Calvert et al., 2000). Recent theoretical (Nguyen et al., 2015; Stone et al., 2018;
578 Peltola et al., 2020) works suggest that the only reaction pathway of the bis-oxy radical important under
579 tropospheric conditions is isomerisation to 'hot' formic acid, followed by decomposition to either H₂ + CO₂ or
580 H₂O + CO, in agreement with experimental and theoretical work on acid pyrolysis experiments (Chang et al.,
581 2007; Vichiatti et al., 2017). Due to the large excess energy and its small size, very little of the hot acid is stabilised,
582 with measured HCOOH yields from ethene ozonolysis < 5% (Calvert et al., 2000) (and the latter may be due to
583 bimolecular reactions of SCI rather than stabilisation of the hot acid). Stone et al. (2018) and Peltola et al. (2020)
584 considered the decomposition of stabilised CH₂OO using master equation simulations, determining the major
585 decomposition channel to be H₂+CO₂ (64 % and 61% respectively), with the H₂O+CO accounting for the
586 remainder (36%) in Stone et al. (2018), while Peltola et al. (2020) also found a small contribution (~8%) from the
587 OH+HCO channel. It is noted that previous experimental work on ethene ozonolysis (Su et al., 1980; Horie et al.,
588 1991; Neeb et al., 1998) has generally inferred a preference for the H₂O+CO channel. This may be due to different
589 pathways being followed by the dioxiranes formed from the excited CH₂OO produced in the ozonolysis reaction
590 compared to those formed from stabilised CH₂OO, as suggested by work on larger systems (Nguyen et al., 2009a;
591 2009b), and in the calculations of Nguyen et al. (2015) on excited CH₂OO decomposition in ethene ozonolysis. A
592 decomposition pathway to HCO + OH, proposed as the source of observed OH yields of 8-15 % in earlier
593 experimental studies on the ozonolysis of ethene (Gutbrod et al., 1997; Rickard et al., 1999; Kroll et al., 2001;
594 Alam et al., 2011) and larger alkenes (Kroll et al., 2002), has recently been determined experimentally to be
595 negligible (Stone et al., 2018), accounting for less than 2 % of the overall decay. This is in agreement with earlier
596 theoretical work (Olzmann et al., 1997; Nguyen et al., 2015) suggesting negligible OH yields from ethene
597 ozonolysis. This apparent discrepancy between experiment and theory can be reconciled by invoking the
598 possibility of OH formation via the carbonyl-hydroperoxide channel in the POZ decomposition, as discussed in
599 Section 2.7.

600 The unimolecular decomposition rate of stabilised CH₂OO has been experimentally determined to be very
601 slow (<12 s⁻¹) (Berndt et al., 2015; Chhantyal-Pun et al., 2015; Newland et al., 2015; Stone et al., 2018; Peltola et
602 al., 2020), with a current recommendation by IUPAC of ≤ 0.2 s⁻¹ at 1 bar and 298 K (Cox et al., 2020). Even at
603 the upper end of these estimates, decomposition is a negligible atmospheric fate for stabilised CH₂OO compared
604 to reaction with water vapour.

605 **4.4 Unimolecular reactions of unsaturated CI**

606 The ozonolysis of conjugated alkenes proceeds via the same initial POZ mechanism as non-conjugated systems,
607 but decomposition of the POZ leads to the formation of unsaturated CI and/or carbonyls. While many of the
608 characteristics of the chemistry are expected to be similar, the theoretical work of Kuwata et al., (2005), Kuwata
609 and Valin (2008), and Vereecken et al. (2017) has shown some important differences. Specifically, additional
610 unimolecular decomposition channels (Figure 7 and Figure 8) become available, which in some cases are faster
611 than the 1,4 H-shift channel.

612



613

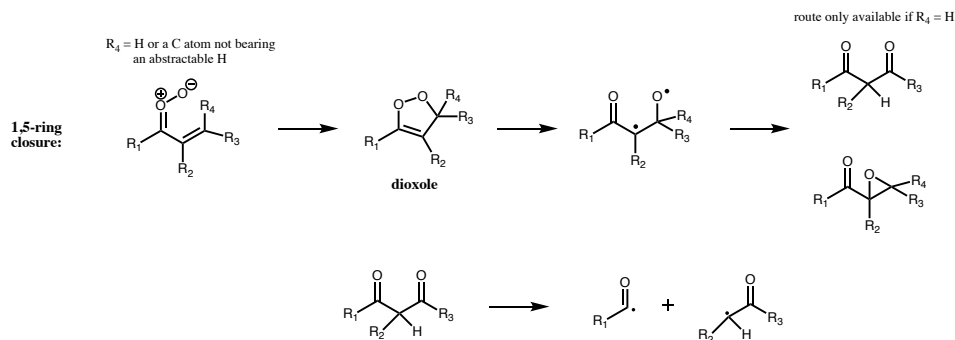
614 **Figure 7. Dominant unimolecular decomposition routes available to unsaturated CI with the terminal oxygen *syn* to an**
615 **α or β vinyl group. Pathways available if terminal oxygen is *anti* to a vinyl group are the same as for saturated CI. For**
616 **1,5-ring closure see Figure 8.**

617 If the vinyl group of an unsaturated CI is *anti* to the terminal oxygen of the carbonyl oxide, then the molecule will
618 follow one of the two routes available to saturated CI, but with a rate affected by the presence of the double bond.
619 However, if the vinyl group is *syn* to the terminal oxygen, alternative mechanisms of decomposition are available.
620 1,4 and 1,6-allyl H-migration (for the vinyl group being in β or α position respectively), are available if an H atom
621 is present on the α or γ carbon. These pathways lead to similar products to 1,4-alkyl H-migration, with a
622 vinylhydroperoxide intermediate decomposing to give OH and one of two possible unsaturated peroxy radicals.
623 If no H-atom is available for (*Z*)- β -unsaturated CI then they follow the 1,3-ring closure channel with SCI
624 decomposition rates $\leq 1 \text{ s}^{-1}$. The rates of the 1,6-allyl H-migration channel for SCI are of the order of 10^6 s^{-1} , while
625 1,4-allyl H-migration of SCI has rates ranging from $10^1 - 10^4 \text{ s}^{-1}$ depending on other substituents (Vereecken et
626 al. 2017).

627 For CI with the carbonyl oxide *syn* to an α vinyl group, and without an available hydrogen on the α
628 carbon, then the dominant decomposition mechanism is 1,5 ring closure, originally proposed by Kuwata et al.
629 (2005) (Figure 8). This forms an intermediate dioxole species with a five membered ring. This is predicted to have
630 high internal energy and to break the O-O bond, leading to an epoxy carbonyl, or, if $R_4 = \text{H}$, to a dicarbonyl
631 (Kuwata 2005). The dicarbonyl has been predicted to undergo further prompt decomposition via various possible
632 unimolecular channels, some of which appear to yield OH (Barber et al., 2018). Based on the stable product
633 distribution from *anti*-MVKO decay, the decomposition of the dicarbonyl has been determined to be
634 predominantly via C-C cleavage leading to two radicals (acetyl and vinoxy radicals in the case of *anti*-MVKO)
635 (Vansco et al., 2020). These radicals will add O_2 leading to RO_2 radicals which may undergo further
636 decomposition if formed chemically excited, ultimately to $\text{HCHO} + \text{OH} + \text{CO}$ in both cases (Carr et al., 2011;
637 Weidman et al., 2018; Vansco et al., 2020). For *syn*-MACRO, Vansco et al. (2020) determine a pathway via a
638 dioxole analogous to that just described, leading to formyl and 2-methyl vinoxy radicals, the latter of which could
639 ultimately yield $\text{CH}_3\text{CHO} + \text{OH} + \text{CO}$. However, this accounts for only about half of the decomposition of the
640 dicarbonyl, with the other half leading to acrolein via an unidentified unimolecular process. It is noted that Barber



641 et al. (2018) and Vansco et al. (2020) did not consider the epoxide isomerisation pathway for the dioxole. The
642 calculated unimolecular decay rates for the dioxole forming pathways from *syn*-MACRO and *anti*-MVKO are
643 fast, Vereecken et al. (2017) reported a rate of $13,400 \text{ s}^{-1}$, while Barber et al. (2018) reported a somewhat slower
644 rate for *anti*-MVKO of 2140 s^{-1} . Decay of stabilized *syn*-MVKO is relatively slow at $33 - 50 \text{ s}^{-1}$ (Vereecken et al.,
645 2017; Barber et al., 2018) making it a potentially important bimolecular reaction partner in the atmosphere.
646



647

648 **Figure 8. 1,5-ring closure: dominant unimolecular pathway for unsaturated CI with the terminal oxygen *syn* to an α**
649 **vinyl group and R_4 is not a carbon with an abstractable hydrogen.**

650 4.5 Protocol Rules for CI decomposition

651 For unimolecular decomposition of CI, the SAR of Vereecken et al. (2017) is used to determine decomposition
652 pathways and rates (for SCI). The products from each decomposition pathway are given in Table 2, where any
653 secondary reactions such as recombination with O_2 are already accounted for. The vinylhydroperoxide pathway
654 is assumed to lead exclusively to a β -oxo alkyl radical and OH. For decomposition via 1,3 ring closure, the hot
655 acid / ester formed is considered to decompose via one of the three major pathways determined for (*E*)-RCHOO:
656 $\text{RH} + \text{CO}_2$ (40%), $\text{ROH} + \text{CO}$ (20%), $\text{R} + \text{HO}_2 + \text{CO}_2$ (40%), based on the observed product yields from *cis* and
657 *trans* but-2-ene experiments by Tuazon et al. (1997). While it is noted that Grosjean et al. (1994) observed a
658 CH_3COOH yield of $\sim 20\%$, this could also be a product of $\text{CH}_3\text{CHOO} + \text{water vapour}$ in their experimental setup.
659 For larger CI ($\geq \text{C}_9$) the acid / ester is considered to be fully stabilised, if two esters can be formed they are
660 considered equally likely. This is recognised as an area where detailed experimental studies are required, to
661 establish the sensitivity of acid / ester stabilisation to CI size, as well as identifying decomposition products for a
662 range of CI sizes / structures, and whether these are different for chemically activated / thermalized dioxiranes, as
663 predicted (Anglada et al., 1998; Nguyen et al., 2009a, 2009b). For CH_2OO decomposition, the protocol assigns
664 the products equally to two decomposition pathways: $\text{H}_2 + \text{CO}_2$ and $\text{H}_2\text{O} + \text{CO}$; as discussed above, no OH is formed
665 directly.

666 For 1,4- and 1,6 allyl H-migration in unsaturated CI (Figure 7), formation of the alkyl radicals from each
667 of the delocalized radical sites formed after OH elimination is assumed to be equally likely. The product yields
668 given in Table 2 are for mechanisms that do not explicitly preserve stereo-specificity. For systems that track
669 stereo-specific substitution on double bonds, H-migration is only possible from the *Z*-substituent, and the number
670 of products is reduced accordingly, with a concomitant adjustment of the product yields.



671 For 1,5 ring closure (Figure 8), formation of the epoxide or the dicarbonyl are considered equally likely.
 672 The dicarbonyl undergoes further decomposition to yield two RO₂ following Barber et al. (2018). Unimolecular
 673 reaction rates for stabilised unsaturated CI are taken from the Vereecken et al. (2017) SAR. Clearly there remains
 674 much uncertainty on the proposed kinetics, and systematic experimental work on SCI yields, and final product
 675 studies of ozonolysis of conjugated alkenes is required to improve the proposed protocol.

676 **Table 2. Decomposition pathways and products for CI in the protocol**

Decomposition Pathway	CI Structure	Products
1,4 H-shift (VHP)		
1,3 ring closure (hot acid / ester) CI < C₉		R ₁ R ₂ + CO ₂ (40 %) R ₁ OR ₂ + CO (20 %) R ₁ + R ₂ + CO ₂ (40 %)
1,3 ring closure (hot acid / ester) CI ≥ C₉		R ₁ CO-O-R ₂ (50%) R ₁ -O-COR ₂ (50%)
CH₂OO		H ₂ +CO ₂ (50 %) H ₂ O+CO (50 %)
1,5-ring closure	R ₄ = H or a C atom not bearing an abstractable H 	
1,5-ring closure (R₃ = H)	R ₄ = H or a C atom not bearing an abstractable H 	(50%) R ₁ C(O)O ₂ + CHOC(O ₂)R ₂ (50%)
1,6 allyl H-shift		(50%) (50%)
1,4 allyl H-shift		(50%) (50%)

677 **5 Bimolecular Reactions of SCI**

678 Based on the unimolecular pathways described in Section 5, many SCI have lifetimes against unimolecular
 679 reaction on the order of 10⁻³ – 10⁻¹ s. These lifetimes are long enough to allow them to participate in bimolecular
 680 reactions with trace gases in the atmosphere under typical boundary layer conditions, where Vereecken et al.
 681 (2017) estimated that just under half of the CI in the atmosphere react with a co-reactant rather than
 682 unimolecularly. The co-reactants for which fast reactions, of potential tropospheric importance, have been
 683 demonstrated are H₂O, (H₂O)₂, SO₂, NO₂, and organic and inorganic acids (Reactions 6 – 11).



686 † only available if $R_2 = H$



692 Reactions with other trace gases have been investigated both experimentally and theoretically, but these are not
693 included in the protocol at this time as they are not considered to be important under tropospheric conditions.
694 Theoretical and experimental work has also shown that more complex bimolecular and unimolecular pathways
695 may operate forming heterocyclic molecules like cyclic peroxides and secondary ozonides (Chuong et al., 2004;
696 Long et al., 2019). Again though, these reactions appear to be of negligible importance in the gas phase for SCI
697 with carbon numbers up to C_{10} (monoterpenes) and are not considered in this protocol. While only reactions
698 relevant to the atmosphere are included in the protocol; reactions that are not expected to be relevant in the
699 atmosphere are still maintained in the database since they may be useful to interpret results of chamber simulations
700 or other laboratory experiments (e.g. self-reaction or reaction with parent alkenes).

701 CH_2OO and (*E*)- $RCHOO$ react rapidly with H_2O (Reaction R6a) (Welz et al., 2012; Taatjes et al., 2013;
702 Stone et al., 2014) and with the water dimer, $(H_2O)_2$, (Reaction R6b) (Berndt et al., 2014a; Chao et al., 2015;
703 Lewis et al., 2015; Lin et al., 2016), such that removal by water vapour is their predominant fate in the atmosphere.
704 However, (*Z*)- $RCHOO$ react slowly with H_2O (Taatjes et al., 2013; Sheps et al., 2014; Huang et al., 2015)
705 increasing the importance of bimolecular reactions with other atmospheric trace species such as acids and SO_2
706 (Newland et al., 2018). The reaction of SCI with organic acids (Reaction R7) is also likely to be an important
707 reaction in the atmosphere (Welz et al., 2014). The experimentally determined reaction rates for SCI + $HCOOH$
708 and CH_3COOH are $1 - 5 \times 10^{-10} \text{ cm}^3 \text{ s}^{-1}$ (Welz et al., 2014; Sipilä et al., 2014; Chung et al., 2019), close to the
709 collisional limit. Other potentially important reactions in the atmosphere include those with SO_2 (Reaction R8),
710 NO_2 (Reaction R9), and inorganic acids (Reactions R10-R11). The rates of SCI+ SO_2 reaction have been the
711 subject of several studies for the three smallest SCI, with good agreement between experiments. Larger SCI appear
712 to have similar reaction rates with SO_2 (Ahrens et al., 2014).

713 The products of many of the bimolecular reactions of SCI are still uncertain. This is the case for the most
714 important bimolecular reactions in the atmosphere, those with H_2O and $(H_2O)_2$. A recent experimental study
715 (Sheps et al., 2017) of the reaction of CH_2OO with the $(H_2O)_2$, generating CH_2OO from the photolysis of
716 diiodomethane, determined yields of: hydroxymethylhydroperoxide (HMHP) (55 %), HCHO (40 %), and
717 $HCOOH$ (5 %). However, ozonolysis experiments (e.g. Nguyen et al., 2016) have generally found HMHP and
718 $HCOOH$ to be the main detected products, with negligible yields of HCHO. Based on results from isoprene
719 ozonolysis chamber experiments, Nguyen et al. (2016) proposed yields from the $CH_2OO + H_2O$ reaction of:
720 HMHP (73 %), $HCOOH$ (21 %), HCHO (6 %); and from the $(H_2O)_2$ reaction of: HMHP (40 %), $HCOOH$ (54 %),
721 HCHO (6 %). These low HCHO yields are in agreement with earlier work (Hasson et al., 2001b) that determined
722 an HCHO yield of 6 – 9 %.



723 The products of SCI reaction with organic acids appear to be mainly hydroperoxide esters (Reaction R7).
724 Hydroperoxy methyl formate (HPMF) has been detected as an intermediate in the $\text{CH}_2\text{OO}+\text{HCOOH}$ reaction (e.g.
725 Neeb et al., 1995; Wolff et al., 1997; Hasson et al., 2001a; Chung et al., 2019), hydroperoxy methyl acetate in the
726 $\text{CH}_2\text{OO}+\text{CH}_3\text{COOH}$ reaction (Neeb et al., 1996), and hydroperoxy ethyl formate in the $\text{CH}_3\text{CHOO}+\text{HCOOH}$
727 reaction (Neeb et al., 1995; 1996; Cabezas and Endo, 2020). Theoretical calculations have predicted the formation
728 of > 90 % HPMF for the reaction of CH_2OO with HCOOH (Vereecken, 2017), and that the production of stabilised
729 hydroperoxide esters will be even higher for larger SCI. The reaction with SO_2 has been shown to form SO_3 with
730 close to unit yield (Reaction R8) (Kuwata et al., 2015). For NO_2 , while early experimental work (Ouyang et al.,
731 2013) suggested SCI would oxidise NO_2 to NO_3 , more recent experimental (Caravan et al., 2017) and theoretical
732 (Vereecken and Nguyen, 2017) work has suggested the formation of a nitroalkylperoxy radical ($\text{R}_1\text{R}_2\text{C}(\text{O}_2)\text{NO}_2$).
733 Subsequent reaction and formation of the alkoxy radical would be expected to yield a carbonyl and NO_2 . The
734 main products of reaction of SCI with the inorganic acid HCl have been predicted to be chlorohydroperoxides
735 (Reaction R10) (Foreman et al., 2016; Vereecken, 2017), with these products observed experimentally for
736 $\text{CH}_2\text{OO}+\text{HCl}$ (Cabezas and Endo, 2017) and $\text{CH}_3\text{CHOO}+\text{HCl}$ (Cabezas and Endo, 2018). The main product of
737 reaction with HNO_3 has been predicted to be hydroperoxynitrates (Reaction R11) (Foreman et al., 2016;
738 Raghunath et al., 2017; Vereecken, 2017). Raghunath et al. (2017) further predicted decomposition of a fraction
739 of the chemically activated hydroperoxynitrates to $\text{CH}_2(\text{O})\text{NO}_3 + \text{OH}$. This reaction has not yet been studied
740 experimentally to the authors' knowledge.

741 5.1 Protocol Rules for SCI Bimolecular Reactions

742 Bimolecular reaction rate coefficients for SCI are included for reaction with water vapour monomers and dimers,
743 SO_2 , NO_2 , carboxylic acids and inorganic acids (HCl , HNO_3) (Table 3). For the water vapour reactions, the rate
744 coefficients are taken from the SAR of Vereecken et al. (2017), which provides values for 98 explicit structures.
745 For bimolecular reactions of SCI with the other trace gases, four classes of SCI are considered: CH_2OO , Z/E -
746 RCHOO and $\text{R}_1\text{R}_2\text{COO}$ (where R represents alkyl groups), based on the limited experimental data available. The
747 rates are taken from IUPAC recommendations (Cox et al., 2020) where available, otherwise from sources as stated
748 in Table 3. Where the structure does not fit into the defined classes, the CH_2OO rate constant is attributed by
749 default. Reaction products are as given in Reactions R6 – R11. In light of the current uncertainties of the product
750 distribution of the reactions of SCI with water, here we assume the same products for the monomer and dimer
751 reactions. We propose yields based on the direct study of Sheps et al. (2017) of α -hydroxyhydroperoxide (55 %),
752 carbonyl (40 %) and acid (5 %), with the exception of $\text{R}_1\text{R}_2\text{COO}$, which cannot form the acid, for which we
753 increase the α -hydroxyhydroperoxide to 60 %. These recommendations will be subject to change upon further
754 experimental information becoming available.

755

756

757

758



759 **Table 3. Bimolecular reaction rates with RCOOH, SO₂, NO₂ and inorganic acids applied to the four SCI structures.**
 760 Rates are IUPAC recommendations (Cox et al., 2020) unless otherwise stated. Bimolecular reaction rates with water
 761 are taken from Vereecken et al. (2017), see main text.

	Bimolecular reaction rates (10 ¹¹ molecules cm ⁻³ s ⁻¹)				
	RC(O)OH	SO ₂	NO ₂	HCl ^a	HNO ₃ ^a
CH ₂ OO	12	3.7	0.3	4.6	54
(<i>E</i>)-RCHOO ^b	38 ^c	14	0.2	4.6	54
(<i>Z</i>)-RCHOO ^b	21 ^c	2.6	0.2	4.6	54
R ₁ R ₂ COO	31	16	0.2	4.6	54

762 ^a All values for CH₂OO reaction from Foreman et al. (2016); ^b IUPAC recommended values for (*E*) and (*Z*)-CH₃CHOO; ^c
 763 Mean of IUPAC recommended values for reaction with HCOOH and CH₃COOH.
 764

765 6 Example of protocol application

766 An example is described below for the unsaturated ketone, 6-methyl-5-hepten-2-one, and illustrated in Figures 9
 767 and 10. Further examples for α -pinene, *cis*-2-pentene, 2-methyl-1-pentene and 2-methyl-1,3-butadiene (isoprene)
 768 are given in the Supplementary (Section S3). The initial rate of reaction with ozone is defined by the protocol in
 769 the companion paper (Jenkin et al., 2020). The branching ratio for formation of the disubstituted CI* is calculated
 770 to be 0.72 using the group additivity values in Table 2 and Eq. (1).
 771

$$772 \quad Y_{CI1} = \frac{(0.218+0.218)-(0+0)+1}{2} = 0.72 = 1 - Y_{CI2} \quad (E3)$$

773

774 The *syn* and *anti*-conformers of the two large CI* are formed with equal yield (0.14).

775 Stabilisation of each CI* is computed using Eq. (2):

776

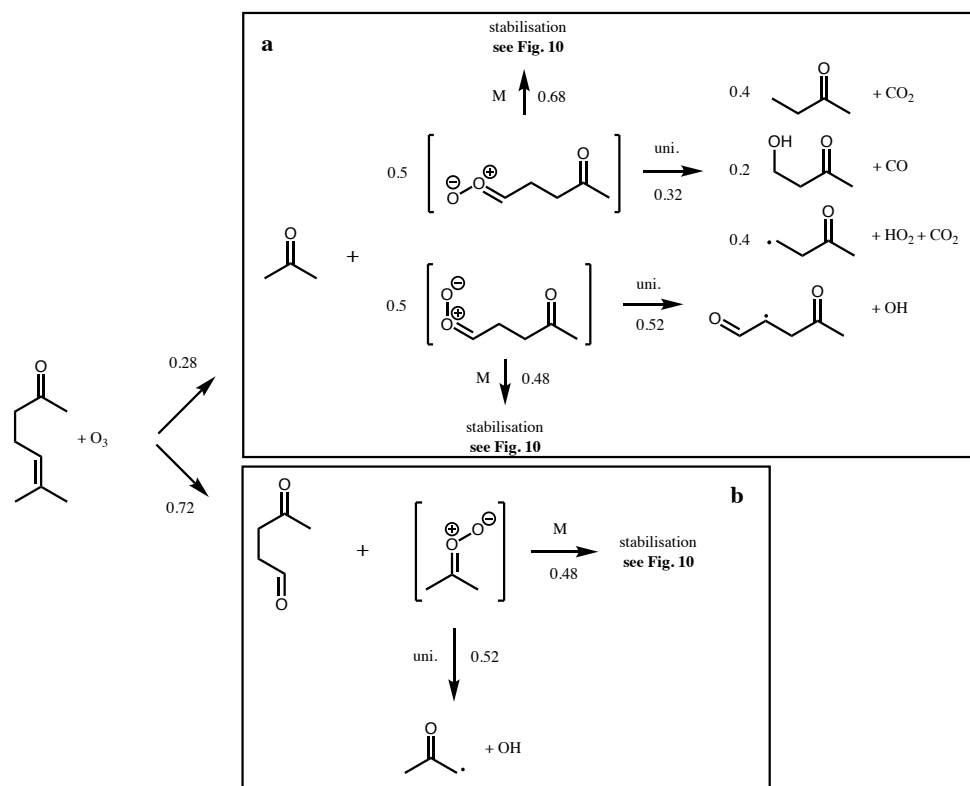
$$777 \quad (CH_3)_2COO: \quad S = 1 - \left[\left(\frac{5}{12} \right) \times 1.242 \times \left(\frac{5}{5+(5-5)} \right) \right] = 0.48 \quad (E4)$$

$$778 \quad (Z)-CH_3C(O)(CH_2)_2CHOO: \quad S = 1 - \left[\left(\frac{8}{12} \right) \times 1.242 \times \left(\frac{5}{8+(5-5)} \right) \right] = 0.48 \quad (E5)$$

$$779 \quad (E)-CH_3C(O)(CH_2)_2CHOO: \quad S = 1 - \left[\left(\frac{8}{12} \right) \times 0.95 \times \left(\frac{5}{8+(5-3)} \right) \right] = 0.68 \quad (E6)$$

780

781 The remaining (CH₃)₂COO* undergoes unimolecular decomposition via the vinylhydroperoxide (VHP) pathway
 782 to yield the acetyl peroxy radical (CH₃C(O)CH₂OO) and OH. The remaining (*Z*)-CH₃C(O)(CH₂)₂CHOO
 783 decomposes via the VHP pathway to yield CH₃C(O)CH₂CH(O₂)CHO + OH, while (*E*)-CH₃C(O)(CH₂)₂CHOO
 784 decomposes via 1,3 ring closure and yields CH₃C(O)CH₂CH₃ + CO₂ (40%), CH₃C(O)CH₂CH₂OH + CO (20%),
 785 CH₃C(O)CH₂CH₂ + H + CO₂ (40%). Each stabilised CI can decompose via the same pathways as its respective
 786 CI*, with temperature dependent rates determined from Vereecken et al. (2017). At 298K these are 478 s⁻¹, 205 s⁻¹
 787 and 74 s⁻¹ for (CH₃)₂COO, (*Z*)-CH₃C(O)(CH₂)₂CHOO and (*E*)-CH₃C(O)(CH₂)₂CHOO respectively.
 788 Alternatively, they can undergo bimolecular reaction. Reaction rates with H₂O and (H₂O)₂ are calculated using
 789 monomer and dimer reaction rates from Vereecken et al. (2017). Reaction rates with other trace gases are taken
 790 from Table 3 for the relevant CI structure. Figure 10 shows calculated pseudo first order reaction rates for reaction
 791 with SO₂ and RCOOH assuming atmospheric mixing ratios of [SO₂] = 5 ppbv and [RCOOH] = 5 ppbv.
 792

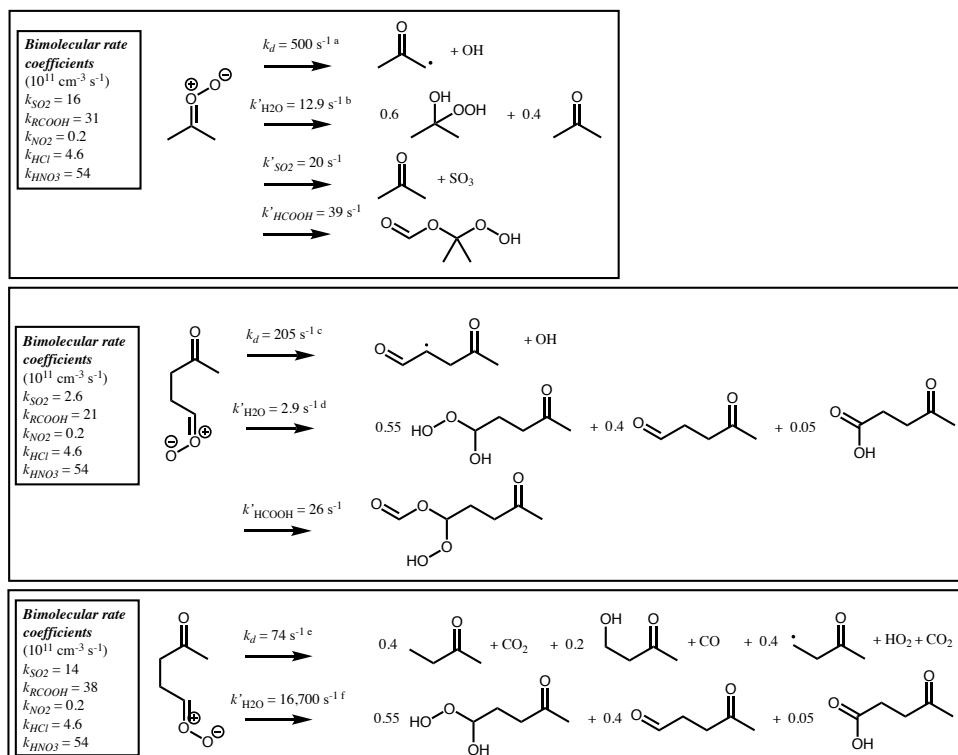


793
 794
 795

Figure 9. Branching ratios and products of the CI decomposition produced following ozonolysis of 6-methyl-5-hepten-2-one



796



797
 798 **Figure 10.** Bimolecular rate coefficients (see Table 3) and products of the SCI produced following ozonolysis of 6-
 799 methyl-5-hepten-2-one at 298 K. Pseudo first order loss rates (k') and products are shown for decomposition and
 800 reaction with water vapour, and for other pathways that contribute more than 1% of the total loss assuming $[\text{SO}_2] = 5$
 801 ppbv, $[\text{RCOOH}] = 5$ ppbv, $[\text{H}_2\text{O}] = 5 \times 10^{17} \text{ cm}^{-3}$, $[(\text{H}_2\text{O})_2] = 5 \times 10^{14} \text{ cm}^{-3}$, $[\text{NO}_2] = 1$ ppbv, $[\text{HCl}] = 100$ pptv, $[\text{HNO}_3] =$
 802 **100 pptv.**

803 ^a $7.64 \times 10^{-60} \times T^{23.59} e^{(2367/T)}$

804 ^b **Sum of first order loss rates to water monomer ($7.54 \times 10^{-18} * [\text{H}_2\text{O}]$) and dimer ($1.82 \times 10^{-14} * [(\text{H}_2\text{O})_2]$)**

805 ^c $2.41 \times 10^{-62} \times T^{24.33} e^{(2571/T)}$

806 ^d **Sum of first order loss rates to water monomer ($1.51 \times 10^{-18} * [\text{H}_2\text{O}]$) and dimer ($4.31 \times 10^{-15} * [(\text{H}_2\text{O})_2]$)**

807 ^e $1.57 \times 10^{10} \times T^{1.03} e^{(-7464/T)}$

808 ^f **Sum of first order loss rates to water monomer ($1.58 \times 10^{-14} * [\text{H}_2\text{O}]$) and dimer ($1.75 \times 10^{-11} * [(\text{H}_2\text{O})_2]$)**

809 7 Protocol Evaluation

810 7.1 Experimental databases and assessment approach

811 A database of experimentally determined carbonyl yields, OH yields and SCI yields has been assembled in order
 812 to evaluate the new protocol (Supplement – Spreadsheets S1-S3). Experimental conditions are also recorded in
 813 the database to enable some assessment of the validity of the assumptions inherent in the experimental setup.

814 The Root Mean Squared Error (RMSE) and the Mean Bias Error (MBE) were examined to assess the
 815 reliability of the protocol. The RMSE and MBE are here defined as:

816

817
$$RMSE = \sqrt{\frac{1}{n} \sum_{i=1}^n (Y_{protocol} - Y_{database})^2} \quad (E7)$$



$$818 \quad MBE = \frac{1}{n} \sum_{i=1}^n (Y_{protocol} - Y_{database}) \quad (E8)$$

819 where n is the number of species in the dataset. The databases were split in to subsets to identify possible bias
 820 within a structural category of species (e.g. exocyclic vs endocyclic monoalkenes). The various subsets examined
 821 and their corresponding number of species are summarized in Table 4. Three databases were used to perform the
 822 protocol assessment: carbonyl yields (Spreadsheet S1), SCI yield (S2), and OH yield (S3). The RMSE and MBE
 823 computed for the full databases and the various subsets are reported in Table 4. The scatter plots of protocol yields
 824 vs database yields, by species category, are given in Figure 11 .

825

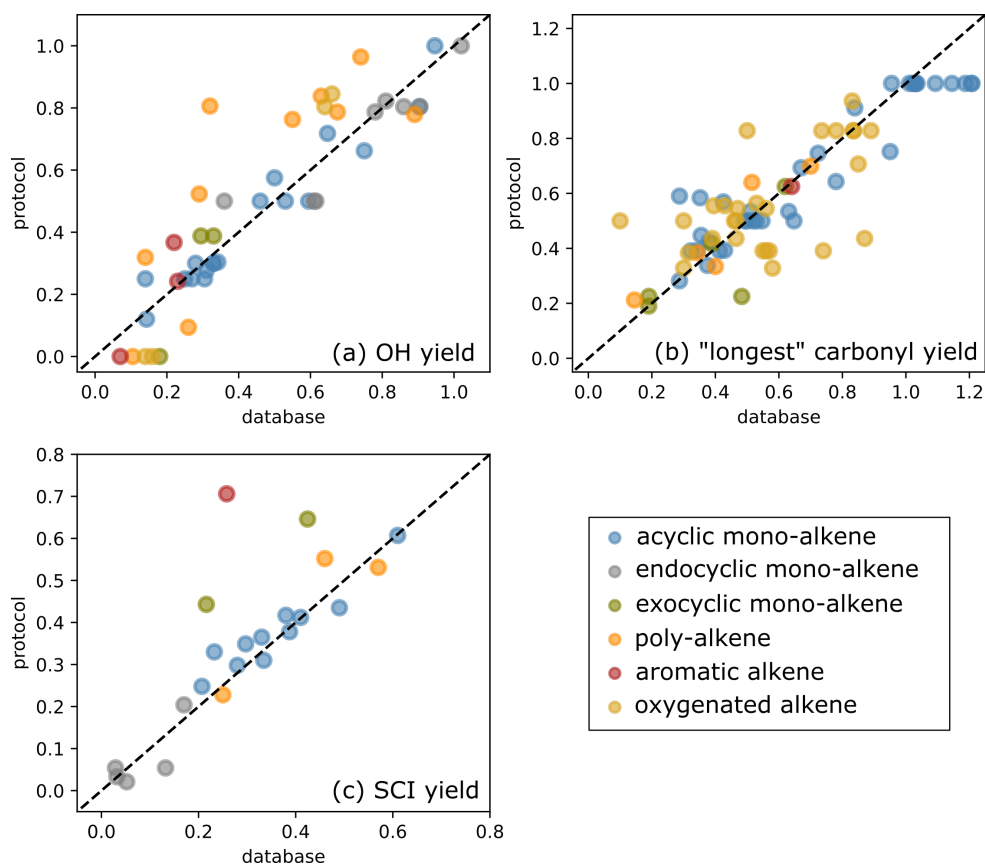
826 **Table 4. Number of species (n) in the database used to compute the mean bias error (MBE) and the root mean square**
 827 **error (RMSE) for the OH yields, SCI yields and "longest" carbonyl yield.**

	all species	acyclic monoalkene	endocyclic monoalkene	exocyclic monoalkene	poly alkene	aromatic alkene	oxygenated alkene
<i>OH yields</i>							
<i>n</i>	46	18	8	3	10	3	4
MBE	0.02	-0.01	-0.03	-0.01	0.13	0.03	0.01
RMSE	0.13	0.06	0.09	0.12	0.23	0.09	0.16
<i>SCI yields</i>							
<i>n</i>	22	11	5	2	3	1	0
MBE	0.05	0.02	-0.01	0.22	0.01	0.45	-
RMSE	0.12	0.04	0.04	0.22	0.06	0.45	-
<i>Yields of the longest carbonyl</i>							
<i>n</i>	73	35	NA [‡]	5	5	1	27
MBE	-0.01	-0.02	-	-0.04	0.03	-0.02	0.00
RMSE	0.14	0.11	-	0.12	0.07	0.02	0.18

828 [‡] Endocyclic alkenes do not produce a stable primary carbonyl as all possible molecules formed from the POZ fragmentation
 829 contain a carbonyl oxide moiety.

830

831



832

833 **Figure 11. Scatter plot of protocol yields vs database yields: (a) OH yields, (b) yields for the "longest" carbonyl and (c)**
834 **SCI yields.**

835 7.2 Primary Carbonyl Yields

836 The primary carbonyl yields from alkene ozonolysis are calculated in the protocol by assigning F values to
837 different functional groups adjacent to the C=C bond that determine the relative fragmentation pattern of the POZ
838 (Section 2). The calculated primary carbonyl yields can be compared to the measurements in the experimental
839 database. For some functional groups however, the number of data available is sparse and the carbonyl yields
840 have been directly used to determine the F value. The carbonyl yields dataset should therefore rather be viewed
841 as a training dataset than a validation dataset in this protocol assessment. Figure 11b shows the scatter plots for
842 the calculated yields of the larger primary carbonyl (i.e. greater number of non-H atoms) formed in POZ
843 decomposition, compared to the experimentally reported values for each alkene in the database. No substantial
844 bias is identified in the computed carbonyl yields (MBE=-0.01). For non-oxygenated alkenes, the fit is reasonably
845 good and the RMSE does not exceed 0.12 for the various hydrocarbon classes reported in Table 4. The major
846 outlier is the yield of 3-methyl-2-pentanone from 3,4-diethyl-2-hexene ozonolysis. This is based on one
847 measurement (Grosjean and Grosjean, 1997). It was noted in Jenkin et al. (2020) that the ozonolysis reaction rate
848 reported by Grosjean and Grosjean (1997) for this compound was a significant outlier from predicted trends, and
849 so it seems possible that this compound was incorrectly identified in the original work. For symmetrical alkenes,



850 the calculated primary carbonyl yield is unity, whereas measured yields tend to cluster slightly above one. This is
851 likely due to a small amount of secondary formation of the carbonyls from bimolecular reactions of SCI. The
852 poorest fitted class is oxygenated alkenes (RMSE=0.18). This is likely due to a combination of factors. Firstly,
853 the majority of these compounds have only one measurement. Secondly, measurements of multi-oxygenated
854 VOCs are known to be more challenging than e.g. simple carbonyls. Thirdly, there is more likely to be additional
855 chemical factors which are not yet understood in the ozonolysis of these more complex molecules influencing the
856 POZ fragmentation. Two of the most significant outliers in the oxygenated alkenes are acrylic and methacrylic
857 acid. As described in Section 2.2.3 it is difficult to reconcile the two available data points.

858 7.3 SCI yields

859 The yield of stabilised Criegee intermediates from an alkene-ozone reaction depends on the alkene structure (i.e.
860 the POZ fragmentation pattern, Section 2), the dominant unimolecular decomposition route of the CI* (Section
861 3.2), and the size of the CI (Section 3.2). The yields calculated by the protocol are independent of the
862 measurements in the database. SCI yields can therefore be considered as a validation dataset to evaluate the
863 reliability of the protocol. Total SCI yields have been measured for a number of alkenes, although the dataset is
864 still relatively small. It should also be noted that many experimentally determined SCI yields have a large
865 uncertainty associated with them, particularly earlier experiments where analysis techniques were less developed
866 and the chemical models lacking. Figure 11c shows the scatter plot of the total SCI yields calculated by the
867 protocol vs experimental data. The data consists predominantly of acyclic monoalkenes, for which there is a good
868 agreement between the measurements and the calculated values (RMSE=0.04). Figure 11c shows three major
869 outliers for which the protocol over-predicts the measured SCI yield. These species are methylene cyclohexane
870 and β -pinene (which constitute the subset of the exocyclic alkenes (RMSE=0.22)) and styrene, the only
871 representative of the aromatic alkenes class in this dataset (RMSE=0.45). The methylene cyclohexane and styrene
872 values are both based on one measurement (Hatakeyama et al., 1984), and the β -pinene value is based on two
873 measurements (Hatakeyama et al., 1984; Newland et al., 2018) which are in poor agreement, giving values of 0.25
874 and 0.60 respectively. This clearly warrants revisiting experimentally, particularly with respect to the
875 atmospherically important monoterpene β -pinene. Finally, the overall protocol SCI yields appear to be biased
876 slightly high (+ 5%), which is mainly explained by the overestimation described above for the exocyclic and
877 aromatic alkenes.

878 7.4 OH yields

879 The reaction of alkenes with ozone yields OH through both primary (i.e. decomposition of CI via a
880 vinylhydroperoxide) and secondary (i.e. peroxy radical chemistry) processes. The primary process can also be
881 split: the decomposition of chemically activated CI*, which under atmospheric conditions (and e.g. chamber
882 laboratory experiment conditions) is assumed to happen at rates such that there is no competition with bimolecular
883 reaction; and the decomposition of stabilised CI, which occurs in competition with bimolecular reactions so that
884 the OH yield depends on the unimolecular rate relative to the concentrations of possible co-reactants. The primary
885 OH yield thus depends on the POZ fragmentation pattern (Section 2) and the decomposition pathways of the CI
886 (Section 3.2).



887 Many studies have measured the OH yield for specific alkene-ozone reactions. As for the SCI yields
888 above, the OH yield database can be viewed as a validation dataset to assess the reliability of the protocol since
889 OH yields are not prescribed explicitly, but are a product of the protocol rules for POZ fragmentation and CI
890 decomposition pathways. For the comparison, protocol yields are computed assuming that all SCI produced
891 undergo unimolecular decomposition (i.e. bimolecular reactions of SCI are ignored). Although many experiments
892 will have been designed in such a way as to try to prevent bimolecular reactions, in reality a small fraction of the
893 SCI will react bimolecularly, not producing OH, so the computed OH yield might be considered an upper limit.
894 On the other hand, in many of the experiments there will likely be some contribution to the measured OH yield
895 from peroxy radical chemistry (e.g. $\text{HO}_2 + \text{O}_3$), making the reported experimental yield an upper limit. No attempt
896 is made here to determine the relative contribution from primary or secondary processes in the reported
897 measurements, which is dependent on both experimental setup and the particular alkene being studied, or to
898 correct for possible bimolecular reactions. Therefore, a comparison between experimental and protocol OH yields
899 clearly carries significant uncertainties.

900 With this in mind, the agreement between computed OH yields and the experimental values is very good
901 (Figure 11a). No substantial bias is observed on the complete dataset (MBE=0.02). It is difficult to comment on
902 some classes as they contain only one or two compounds (see Table 4). The protocol appears especially reliable
903 for estimating the OH yields for monoalkenes (RMSE=0.06) and endocyclic alkenes (RMSE=0.09). The class for
904 which the protocol does worst is polyalkenes (RMSE=0.23), with a systematic over-prediction at higher OH yields
905 (MBE=0.13). There are five compounds for which the protocol calculates an OH yield of zero (styrene, 1,3-
906 butadiene, methyl vinyl ketone, methacrolein, and camphene). The measured OH yields of these compounds are
907 all below 0.2 and the measured OH could be a result of peroxy radical chemistry.

908 8 Conclusions

909 This manuscript provides a protocol by which the central features of alkene ozonolysis chemistry can be included
910 in an explicit automatic chemical mechanism generator. It also serves to highlight the many gaps that remain in
911 our knowledge of this complex, atmospherically important, process. This will hopefully help direct both
912 experimental and theoretical research towards improving understanding in these areas. Some of the major areas
913 of uncertainty identified in this work include:

- 914 (i) The impact of oxygenated substituents on POZ fragmentation
- 915 (ii) The impact of alkene structure on (*E*)/(*Z*)-CI conformer yields
- 916 (iii) Products of the hot acid / ester channel and trends in the stabilisation of the hot acid / ester with size
- 917 (iv) Further details of the mechanisms and products of non-Criegee ozonolysis chemistry, e.g. step-wise
918 decomposition of the POZ via a carbonyl hydroperoxide
- 919 (v) Product distributions of some of the major atmospheric SCI bimolecular reactions – e.g. the reaction
920 of (*Z*)-RCHO / CH_2OO with H_2O / $(\text{H}_2\text{O})_2$
- 921 (vi) Experimental evidence of the products of conjugated alkene ozonolysis
- 922 (vii) Data on OH and SCI yields from alkenes with (multiple) functional groups
- 923
- 924

925 The reliability of the protocol designed in this work was assessed using experimental values for the OH, SCI and
926 primary carbonyl yields. For these three datasets, the Mean Bias Error (MBE) for the protocol based yields is



927 below 0.05, with no substantial bias identified. The protocol currently provides a fairly reliable estimate of the
928 OH, SCI and primary carbonyl yields with Root Mean Squared Errors (RMSE) of 0.12, 0.13 and 0.15,
929 respectively. However, the number of data available for some classes of compounds remains limited, such as
930 oxygenated, exocyclic and poly-alkenes. The errors in the yields calculated for these species are also the most
931 substantial, and additional experimental data for these categories of compound would be highly valuable to
932 improve the protocol and its assessment.

933 Acknowledgements

934 This work was performed as part of the MAGNIFY project, with funding from the French National Research Agency (ANR)
935 under project ANR-14-CE01-0010, and the UK Natural Environment Research Council (NERC) via grant NE/M013448/1. It
936 was also partially funded by the European Commission (EUROCHAMP-2020 (grant no. 730997)) and the UK National Centre
937 for Atmospheric Sciences (NCAS) Air Pollution Theme.

938 Special issue statement

939 This article is part of the special issue “Simulation chambers as tools in atmospheric research (AMT/ACP/GMD inter-journal
940 SI)”. It is not associated with a conference.

941 References

- 942 Ahrens, J., Carlsson, P. T. M., Hertl, N., Olzmann, M., Pfeifle, M., Wolf, J. L., and Zeuch, T.: Infrared Detection of Criegee
943 Intermediates Formed during the Ozonolysis of β -pinene and Their Reactivity towards Sulfur Dioxide, *Angew. Chem.*, 53,
944 715–719, 2014.
- 945 Alam, M. S., Camredon, M., Rickard, A. R., Carr, T., Wyche, K. P., Hornsby, K. E., Monks, P. S., and Bloss, W. J.: Total
946 radical yields from tropospheric ethene ozonolysis, *Phys. Chem. Chem. Phys.*, 13, 11002–11015, 2011.
- 947 Almatarneh, M. H., Elayan, I. A., Altarawneh, M., and Hollett, J. W.: A computational study of the ozonolysis of sabinene,
948 *Theor. Chem. Acc.*, 138, Article No. 30, 2019.
- 949 Al Mulla, I., Viera, L., Morris, R., Sidebottom, H., Treacy, J., and Mellouki, A.: Kinetics and Mechanisms for the Reactions
950 of Ozone with Unsaturated Oxygenated Compounds, *Chem. Phys. Chem.*, 11, 4069–4078, 2010.
- 951 Anglada, J. M., Bofill, J. M., Olivella, S., and Solé, A.: Theoretical Investigation of the Low-Lying Electronic States of
952 Dioxirane: Ring Opening to Dioxymethane and Dissociation into CO₂ and H₂, *J. Phys. Chem. A*, 102, 3398–3406, 1998.
- 953 Anglada, J. M., Crehuet, R., and Bofill, J. M.: The Ozonolysis of Ethylene: A Theoretical Study of the Gas-Phase Reaction
954 Mechanism, *Chem. Eur. J.*, 5, 1809–1822, 1999.
- 955 Aschmann, S. M., Tuazon, E. C., Arey, J., and Atkinson, R.: Products of the Gas-Phase Reaction of O₃ with Cyclohexene, *J.*
956 *Phys. Chem. A*, 107, 2247–2255, 2003.
- 957 Atkinson, R., and Aschmann, S. M.: OH radical production from the gas-phase reactions of O₃ with a series of alkenes under
958 atmospheric conditions, *Environ. Sci. Technol.*, 27, 1357–1363, 1993.
- 959 Atkinson, R., Baulch, D. L., Cox, R. A., Crowley, J. N., Hampson, R. F., Hynes, R. G., Jenkin, M. E., Rossi, M. J., Troe, J.,
960 and IUPAC Subcommittee: Evaluated kinetic and photochemical data for atmospheric chemistry: Volume II – gas phase
961 reactions of organic species, *Atmos. Chem. Phys.*, 6, 3625–4055, <https://doi.org/10.5194/acp-6-3625-2006>, 2006.
- 962 Aumont, B., Szopa, S., and Madronich, S.: Modelling the evolution of organic carbon during its gas-phase tropospheric
963 oxidation: development of an explicit model based on a self generating approach, *Atmos. Chem. Phys.*, 5, 2497–2517,
964 <https://doi.org/10.5194/acp-5-2497-2005>, 2005.



- 965 Barber, V. P., Shubhrangshu, P., Green, A. M., Trongsirivat, N., Walsh, P. J., Klippenstein, S. J., and Lester, M. I.: Four-
966 Carbon Criegee Intermediate from Isoprene Ozonolysis: Methyl Vinyl Ketone Oxide Synthesis, Infrared Spectrum, and OH
967 Production, *J. Am. Chem. Soc.*, 140, 10866-10880, 2018.
- 968 Barber, V. P., Hansen, A. S., Georgievskii, Y., Klippenstein, S. J., and Lester, M. I.: Experimental and theoretical studies of
969 the doubly substituted methyl-ethyl Criegee intermediate : Infra-red action spectroscopy a unimolecular decay to OH radical
970 products, *J. Chem. Phys.*, 152, 094301, doi:10.1063/5.0002422, 2020.
- 971 Barnes, I., Zhou, S.M., Klotz, B.: In Final Report of the EU project MOST, Contract EVK2-CT-2001-00114. European Union,
972 Brussels, 2005.
- 973 Bauld, N. L., Thompson, J. A., Hudson, C. E., and Bailey, P. S.: Stereospecificity in Ozonide and Cross-Ozonide Formation,
974 *J. Am. Chem. Soc.*, 90, 1822-1830, 1968.
- 975 Bernard, F., Eglunent, G., Daële, V., and Mellouki, A.: Kinetics and Products of Gas-Phase Reactions of Ozone with Methyl
976 Methacrylate, Methyl Acrylate, and Ethyl Acrylate, *J. Phys. Chem. A*, 114, 8376–8383, 2010.
- 977 Berndt, T., Voigtländer, J., Stratmann, F., Junninen, H., Mauldin III, R. L., Sipilä, M., Kulmala, M., and Herrmann, H.:
978 Competing atmospheric reactions of CH₂OO with SO₂ and water vapour, *Phys. Chem. Chem. Phys.*, 16, 19130–19136, 2014a.
- 979 Berndt, T., Jokinen, T., Sipilä, M., Mauldin III, R. L., Herrmann, H., Stratmann, F., Junninen, H., and Kulmala, M.: H₂SO₄
980 formation from the gas-phase reaction of stabilized Criegee intermediates with SO₂: Influence of water vapour content and
981 temperature, *Atmos. Environ.*, 89, 603-612, 2014b.
- 982 Berndt, T., Kaethner, R., Voigtländer, J., Stratmann, F., Pfeifle, M., Reichle, P., Sipilä, M., Kulmala, M., and Olzmann, M.:
983 Kinetics of the unimolecular reaction of CH₂OO and the bimolecular reactions with the water monomer, acetaldehyde and
984 acetone under atmospheric conditions, *Phys. Chem. Chem. Phys.*, 17, 19862–19873, 2015.
- 985 Bey, I., Aumont, B., and Toupance, G: The nighttime production of OH radicals in the continental troposphere, *Geophys. Res.*
986 *Letts*, 24, 1067-1070, 1997.
- 987 Cabezas, C., and Endo, Y.: Spectroscopic Characterization of the Reaction Products between the Criegee Intermediate CH₂OO
988 and HCl, *Chem. Phys. Chem.*, 18, 1860-1863, 2017.
- 989 Cabezas, C., and Endo, Y.: The reaction between the methyl Criegee intermediate and hydrogen chloride: an FTMW spectroscopic
990 study, *Phys. Chem. Chem. Phys.*, 20, 22569-22575, 2018.
- 991 Cabezas, C., and Endo, Y.: Observation of hydroperoxyethyl formate from the reaction between the methyl Criegee intermediate and
992 formic acid, *Phys. Chem. Chem. Phys.*, 22, 446-454, 2020.
- 993 Calvert, J. G., Atkinson, R., Kerr, J. A., Madronich, S., Moortgat, G. K., Wallington, T. J., and Yarwood, G.: *The Mechanism of*
994 *Atmospheric Oxidation of the Alkenes*, Oxford University Press, New York, USA, 552 pp., 2000.
- 995 Campos-Pineda, M. and Zhang, J.: Product yields of stabilized Criegee intermediates in the ozonolysis reactions of *cis*-2-
996 butene, 2-methyl-2-butene, cyclopentene, and cyclohexene, *Science China Chemistry*, 61, 850-856, 2018.
- 997 Caravan, R. L., Khan, A. H. M., Rotavera, B., Papajak, E., Antonov, I. O., Chen, M. -W., Au, K., Chao, W., Osborn, D. L.,
998 Lin, J. J. -M., Percival, C. J., Shallcross, D. E., and Taatjes, C. E.: Products of Criegee intermediate reactions with NO₂:
999 experimental measurements and tropospheric implications, *Faraday Discuss.*, 200, 313-330, 2017.
- 1000 Caravan, R. L., Vansco, M. F., Au, K., Khan, M. A. H., Li, Y. L., Winiberg, F. A., ... & Lester, M. I.: Direct kinetic
1001 measurements and theoretical predictions of an isoprene-derived Criegee intermediate. *Proceedings of the National Academy*
1002 *of Sciences*, 117(18), 9733-9740, 2020.
- 1003 Carr, S. A., Glowacki, D. R., Liang, C. -H., Baeza-Romero, M. T., Blitz, M. A., Pilling, M. J., and Seakins, P. W.: Experimental
1004 and Modeling Studies of the Pressure and Temperature Dependences of the Kinetics and the OH Yields in the Acetyl + O₂
1005 Reaction, *J. Phys. Chem. A*, 115, 1069–1085, 2011.
- 1006 Carslaw, N.: A new detailed chemical model for indoor air pollution, *Atmos. Environ.*, 41, 1164-1179, 2007.
- 1007 Chang, J. -G., Chen, H. -T., Xu, S., and Lin, M. C.: Computational study on the kinetics and mechanisms for the unimolecular
1008 decomposition of formic and oxalic acids, *J. Phys. Chem. A*, 111, 6789–6797, 2007.



- 1009 Chao, W., Hsieh, J. -T., Chang C.-H., and Lin J. J. -M.: Direct kinetic measurement of the reaction of the simplest Criegee
1010 intermediate with water vapour, *Science*, 347, 751–754, doi:10.1126/science.1261549, 2015.
- 1011 Chen, B. -Z., Anglada, J. M., Huang, M. -B., and Kong, F.: The Reaction of CH_2 (X^3B_1) with O_2 ($X^3\Sigma_g^-$): A Theoretical
1012 CASSCF/CASPT2 Investigation, *J. Phys. Chem. A*, 106, 1877–1884, 2002.
- 1013 Chhantyal-Pun, R., Davey, A., Shallcross, D. E., Percival, C. J., and Orr-Ewing, A. J.: A kinetic study of the CH_2OO Criegee
1014 intermediate self-reaction, reaction with SO_2 and unimolecular reaction using cavity ring-down spectroscopy, *Phys. Chem.*
1015 *Chem. Phys.*, 17, 3617–3626, 2015.
- 1016 Chhantyal-Pun, R., Khan, M. A. H., Taatjes, C. A., Percival, C. J., Orr-Ewing, A. J., and Shallcross, D. E.: Criegee
1017 intermediates: production, detection and reactivity, *Int. Rev. Phys. Chem.*, 39, 385-424, 2020.
- 1018 Chung, C. -A., Su, J. W., and Lee, Y. -P.: Detailed mechanism and kinetics of the reaction of Criegee intermediate CH_2OO
1019 with HCOOH investigated *via* infrared identification of conformers of hydroperoxymethyl formate and formic acid anhydride,
1020 *Phys. Chem. Chem. Phys.*, 21, 21445–21455, 2019.
- 1021 Chuong, B., Zhang, J., and Donahue, N. M.: Cycloalkene Ozonolysis: Collisionally Mediated Mechanistic Branching, *J. Am.*
1022 *Chem. Soc.*, 126, 12363–12373, 2004.
- 1023 Cremer, D.: Stereochemistry of the Ozonolysis of Alkenes: Ozonide versus Carbonyl Oxide Control, *Angew. Chem.*, 20,
1024 888-889, 1981.
- 1025 Cox, R. A., Ammann, M., Crowley, J. N., Herrmann, H., Jenkin, M. E., McNeill, V. F., Mellouki, A., Troe, J., and Wallington,
1026 T. J.: Evaluated kinetic and photochemical data for atmospheric chemistry: Volume VII – Criegee intermediates, *Atmos.*
1027 *Chem. Phys.*, 20, 13497-13519, 2020.
- 1028 Cremer, D.: Theoretical Determination of Molecular Structure and Conformation. 8. Energetics of the Ozonolysis Reaction.
1029 Primary Ozonide vs. Carbonyl Oxide Control of Stereochemistry, *J. Am. Chem. Soc.*, 103, 3627-3633, 1981.
- 1030 Drozd, G. T., Kroll, J., and Donahue, N. M.: 2,3-Dimethyl-2-butene (TME) ozonolysis: Pressure dependence of stabilized
1031 criegee intermediates and evidence of stabilized vinyl hydroperoxides, *J. Phys. Chem. A*, 115, 161-166, 2011.
- 1032 Drozd, G. T., and Donahue, N. M.: Pressure dependence of stabilized Criegee intermediate formation from a sequence of
1033 alkenes, *J. Phys. Chem. A*, 115, 4381-4387, 2011.
- 1034 Drozd, G. T., Kurtén, T., Donahue, N. M., Lester, M. I.: Unimolecular decay of the dimethyl-substituted criegee intermediate
1035 in alkene ozonolysis: Decay time scales and the importance of tunnelling, *J. Phys. Chem. A*, 121, 6036-6045, 2017.
- 1036 Ehn, M., Thornton, J. A., Kleist, E., Sipilä, M., Junninen, H., Pullinen, I., Springer, M., Rubach, F., Tillmann, R., Lee, B.,
1037 Lopez-Hilfiker, F., Andres, S., Acir, I.-H., Rissanen, M., Jokinen, T., Schobesberger, S., Kangasluoma, J., Kontkanen, J.,
1038 Nieminen, T., Kurtein, T., Nielsen, L. B., Jørgensen, S., Kjaergaard, H. G., Canagaratna, M., Maso, M. D., Berndt, T., Petäjä,
1039 T., Wahner, A., Kerminen, V.-M., Kulmala, M., Worsnop, D. R., Wildt, J., and Mentel, T. F.: A large source of low-volatility
1040 secondary organic aerosol, *Nature*, 506, 476–479, <https://doi.org/10.1038/nature13032>, 2014.
- 1041 Elshorbany, Y. F., Kurtenbach, R., Wiesen, P., Lissi, E., Rubio, M., Villena, G., Gramsch, E., Rickard, A. R., Pilling, M. J.,
1042 and Kleffmann, J.: Oxidation capacity of the city air of Santiago, Chile, *Atmos. Chem. Phys.*, 9, 2257–2273,
1043 <https://doi.org/10.5194/acp-9-2257-2009>, 2009.
- 1044 Emmerson, K. M., Carslaw, N., and Pilling, M. J.: Urban Atmospheric Chemistry During the PUMA Campaign 2: Radical
1045 Budgets for OH, HO_2 and RO_2 , *J. Atmos. Chem.*, 52, 165-183, 2005.
- 1046 Fenske, J. D., Hasson, A. S., Paulson, S. E., Kuwata, K. T., Ho, A., and Houk, K. N.: The Pressure Dependence of the OH
1047 Radical Yield from Ozone-Alkene Reactions, *J. Phys. Chem. A*, 104, 7821-7833, 2000.
- 1048 Fliszár, S., and Granger, M.: A Quantitative Investigation of the Ozonolysis Reaction: XI. On the Effects of Substituents in
1049 Directing the Ozone Cleavage of trans-1,2-Disubstituted Ethylenes, *J. Am. Chem. Soc.*, 92, 3361-3369, 1970.
- 1050 Fliszár, S., and J., Renard: Quantitative investigation of the ozonolysis reaction. XIV. A simple carbonium ion stabilization
1051 approach to the ozone cleavage of unsymmetrical olefins, *J. Am. Chem. Soc.*, 93, 6953-6963, 1970.



- 1052 Fliszár, S., J., Renard, and Simon, D. Z.: A Quantitative Investigation of the Ozonolysis Reaction. XV. Quantum Chemical
1053 Interpretation of the Substituent Effects on the Cleavage of 1,2,3-Trioxolanes, *J. Am. Chem. Soc.*, 93, 6953-6963, 1971.
- 1054 Foreman, E. S., Kapnas, K. M., and Murray, C.: Reactions between Criegee Intermediates and the inorganic Acids HCl and
1055 HNO₃: Kinetics and Atmospheric Implications, *Angew. Chem. Int. Ed. Engl.*, 55, doi:10.1002/anie.201604662, 2016.
- 1056 Grosjean, D., Williams, E. L., and Grosjean, E.: Atmospheric chemistry of isoprene and of its carbonyl products, *Environ. Sci.*
1057 *Technol.*, 27, 830-840, 1993.
- 1058 Grosjean, D., Williams, E. L., Grosjean, E., Andino, J. M., and Seinfeld, J. H.: Atmospheric oxidation of biogenic
1059 hydrocarbons: reaction of ozone with β -pinene, d-limonene and trans-caryophyllene, *Environ. Sci. Technol.*, 27, 2754-2758,
1060 1993.
- 1061 Grosjean, D., Grosjean, E., and Williams, E. L.: Atmospheric Chemistry of Olefins: A Product Study of the Ozone-Alkene
1062 Reaction with Cyclohexane Added to Scavenge OH, *Environ. Sci. Technol.*, 28, 188-196, 1994.
- 1063 Grosjean, E., Grosjean, D., and Seinfeld, J. H.: Gas phase reaction of ozone with trans-2-hexenal, trans-2-hexenyl acetate,
1064 ethylvinyl ketone and 6-methyl-5-hepten-2-one, *Int. J. Chem. Kinet.*, 28, 373-382, 1996.
- 1065 Grosjean, E., and Grosjean, D.: The Gas Phase Reaction of Unsaturated Oxygenates with Ozone: Carbonyl Products and
1066 Comparison with the Alkene-Ozone Reaction, *J. Atmos. Chem.*, 27, 271-289, 1997.
- 1067 Grosjean, E., and Grosjean, D.: The Reaction of Unsaturated Aliphatic Oxygenates with Ozone, *J. Atmos. Chem.*, 32, 205-
1068 232, 1999.
- 1069 Gutbrod, R., Meyer, S., Rahman, M. M., and Schindler, R. N.: On the use of CO as scavenger for OH radicals in the ozonolysis
1070 of simple alkenes and isoprene, *Int. J. Chem. Kinet.*, 29, 717-723, 1997.
- 1071 Hakala, J. P., and Donahue, N. M.: Pressure-Dependent Criegee Intermediate Stabilization from Alkene Ozonolysis, *J. Phys.*
1072 *Chem. A*, 120, 2173-2178, 2016.
- 1073 Hakala, J. P., and Donahue, N. M.: Pressure Stabilization of Criegee Intermediates Formed from Symmetric trans-Alkene
1074 Ozonolysis, *J. Phys. Chem. A*, 122, 9426-9434, 2018.
- 1075 Hakola, H., Arey, J., Aschmann, S. M., and Atkinson, R.: Product formation from the gas-phase reactions of OH radicals and
1076 O₃ with a series of monoterpenes, *J. Atmos. Chem.*, 18, 75-102, 1994.
- 1077 Hasson, A. S., Orzechowska, G., and Paulson, S. E.: Production of stabilized Criegee intermediates and peroxides in the gas
1078 phase ozonolysis of alkenes 1. Ethene, trans-2-butene, and 2,3- dimethyl-2-butene, *J. Geophys. Res.*, 106, 34131-34142,
1079 2001a.
- 1080 Hasson, A. S., Ho, A. W., Kuwata, K., and Paulson, S. E.: Production of stabilized Criegee intermediates and peroxides in the
1081 gas phase ozonolysis of alkenes 2. Asymmetric and biogenic alkenes, *J. Geophys. Res.*, 106, 34143-34153, 2001b.
- 1082 Hatakeyama, S., Kobayashi, H., and Akimoto, H.: Gas-phase oxidation of sulfur dioxide in the ozone-olefin reactions, *J. Phys.*
1083 *Chem.* 88, 4736-4739, 1984.
- 1084 Heard, D. E., Carpenter, L. J., Creasey, D. J., Hopkins, J. R., Lee, J. R., Lewis, A. C., Pilling, M. J., Seakins, P. W., Carslaw,
1085 N., and Emmerson, K. M.: High levels of the hydroxyl radical in the winter urban troposphere, *Geophys. Res. Lett.*, 31,
1086 L18112, 2004.
- 1087 Herron, J. T., and Huie, R. E. Stopped-flow studies of the mechanisms of ozone-alkene reactions in the gas phase: propene
1088 and isobutene, *J. Am. Chem. Soc.*, 99, 5430-5435, 1977.
- 1089 Herron, J. T., and Huie, R. E. Stopped-flow studies of the mechanisms of ozone-alkene reactions in the gas phase. I. Ethylene,
1090 *J. Am. Chem. Soc.*, 99, 5430-5435, 1978.
- 1091 Huang, H. -L., Chao, W., and Lin, J. J. -M.: Kinetics of a Criegee intermediate that would survive at high humidity and may
1092 oxidize atmospheric SO₂, *Proc. Natl. Acad. Sci.*, 112, 10857-10862, 2015.
- 1093 Iyer, S., Rissanen, M. P., Valiev, R., Barua, S., Krechmer, J. E., Thornton, J., Ehn, M., and Kurtén, T.: Molecular mechanism
1094 for rapid autoxidation in α -pinene ozonolysis, *Nat. Comms.*, 12, doi.org/10.1038/s41467-021-21172-w, 2021.
- 1095 Jenkin, M. E., Saunders, S. M., and Pilling, M. J.: The tropospheric degradation of volatile organic compounds: a protocol for
1096 mechanism development, *Atmos. Environ.*, 31, 81-104, 1997.



- 1097 Jenkin, M. E., Young, J. C., and Rickard, A. R.: The MCM v3.3.1 degradation scheme for isoprene, *Atmos. Chem. Phys.*, 15,
1098 11433-11459, 2015.
- 1099 Jenkin, M. E., Valorso, R., Aumont, B., Rickard, A. R., and Wallington, T. J.: Estimation of rate coefficients and branching
1100 ratios for gas-phase reactions of OH with aliphatic organic compounds for use in automated mechanism construction, *Atmos.*
1101 *Chem. Phys.*, 18, 9297–9328, <https://doi.org/10.5194/acp-18-9297-2018>, 2018a.
- 1102 Jenkin, M. E., Valorso, R., Aumont, B., Rickard, A. R., and Wallington, T. J.: Estimation of rate coefficients and branching
1103 ratios for gas-phase reactions of OH with aromatic organic compounds for use in automated mechanism construction, *Atmos.*
1104 *Chem. Phys.*, 18, 9329–9349, <https://doi.org/10.5194/acp-18-9329-2018>, 2018b.
- 1105 Jenkin, M. E., Valorso, R., Aumont, B., and Rickard, A. R.: Estimation of rate coefficients and branching ratios for reactions
1106 of organic peroxy radicals for use in automated mechanism construction, *Atmos. Chem. Phys.*, 19, 7691–7717,
1107 <https://doi.org/10.5194/acp-19-7691-2019>, 2019.
- 1108 Jenkin, M. E., Valorso, R., Aumont, B., Newland, M. J., and Rickard, A. R.: Estimation of rate coefficients for the reactions
1109 of O₃ with unsaturated organic compounds for use in automated mechanism construction, *Atmos. Chem. Phys.*, 20, 12921-
1110 12937, 2020.
- 1111 Johnson, D. and Marston, G.: The gas-phase ozonolysis of unsaturated volatile organic compounds in the troposphere, *Chem.*
1112 *Soc. Rev.*, 37, 699–716, 2008.
- 1113 Kalalian, C., Roth, E., El Dib, G., Singh, H. J., Rao, P. K., and Chakir, A.: Product investigation of the gas phase ozonolysis
1114 of 1-penten-3-ol, *cis*-2-penten-1-ol and *trans*-3-hexen-1-ol, *Atmos. Environ.*, 238, 117732, 2020.
- 1115 Kalberer, M., Yu, J., Cocker, D. R., Flagan, R. C., and Seinfeld, J. H.: Aerosol Formation in the Cyclohexene-Ozone System,
1116 *Environ. Sci. Technol.*, 34, 4894-4901, 2000.
- 1117 Kidwell, N. M., Li, H., Wang, X., Bowman, J. M., and Lester, M. I.: Unimolecular dissociation dynamics of vibrationally
1118 activated CH₃CHOO Criegee intermediates to OH radical products, *Nat. Chem.*, 8, 509-514, 2016.
- 1119 Klotz, B., Barnes, I., and Imamura, T.: Product study of the gas phase reactions of O₃, OH and NO₃ reactions with methyl
1120 vinyl ether, *Phys. Chem. Chem. Phys.*, 6, 1725–1734, 2004.
- 1121 Kristensen, K., Cui, T., Zhang, H., Gold, A., Glasius, M., and Surratt, J. D.: Dimers in α -pinene secondary organic aerosol:
1122 effect of hydroxyl radical, ozone, relative humidity and aerosol acidity, *Atmos. Chem. Phys.*, 14, 4201–4218, 2014.
- 1123 Kroll, J. H., Hanisco, T. F., Donahue, N. M., Demerjian, K. L., and Anderson, J. G.: Accurate, direct measurements of OH
1124 yields from gas-phase ozone-alkene reactions using an in-situ LIF instrument, *Geophys. Res. Lett.*, 28, 3863-3866, 2001.
- 1125 Kroll, J., Donahue, N. M., Cee, V. J., Demerjian, K. L., and Anderson, J. G.: Gas-phase ozonolysis of alkenes: Formation of
1126 OH from anti carbonyl oxides, *J. Am Chem. Soc.*, 124, 8518-8519, 2002.
- 1127 Kuwata, K. T., Valin, L. C., and Converse, A. D.: Quantum chemical and master equation studies of the methyl vinyl carbonyl
1128 oxides formed in isoprene ozonolysis, *J. Phys. Chem. A*, 109, 10710-10725, 2005.
- 1129 Kuwata, K. T., and Valin, L. C.: Quantum chemical and RRKM/master equation studies of isoprene ozonolysis: Methacrolein
1130 and methacrolein oxide, *Chem. Phys. Lett.*, 451, 186-191, 2008.
- 1131 Kuwata, K. T., Guinn, E. J., Hermes, M. R., Fernandez, J. A., Mathison, J. M., and Huang, K. A.: Computational Re-
1132 examination of the Criegee Intermediate-Sulfur Dioxide Reaction, *J. Phys. Chem. A*, 119, 10316-10335, 2015.
- 1133 Kuwata, K. T., Luu, L., Weberg, A. B., Huang, K., Parsons, A. J., Peebles, L. A., Rackstraw, N. B., and Kim, M. J.: Quantum
1134 Chemical and Statistical Rate Theory Studies of the Vinyl Hydroperoxides Formed in *trans*-2-Butene and 2,3-Dimethyl-2-
1135 butene Ozonolysis, *J. Phys. Chem. A*, 122, 2485-2502, 2018.
- 1136 Lee, A., Goldstein, A. H., Keywood, M. D., Gao, S., Varutbangkul, V., Bahreini, R., Ng, N. L., Flagan, R. C., and Seinfeld, J.
1137 H.: Gas-phase products and secondary organic aerosol yields from the ozonolysis of ten different terpenes, *J. Geophys. Res.*,
1138 111, D07302, 2006.
- 1139 Le Person, A., Solignac, G., Oussar, F., Daële, V., Mellouki A., Winterhalter, R., and Moortgat, G. K.: Gas phase reaction of
1140 allyl alcohol (2-propen-1-ol) with OH radicals and ozone, *Phys. Chem. Chem. Phys.*, 11, 7619–7628, 2009.



- 1141 Lewin, A. G., Johnson, D., Price, D. W., and Marston, G.: Aspects of the kinetics and mechanism of the gas-phase reactions
1142 of ozone with conjugated dienes, *Phys. Chem. Chem. Phys.*, 3, 1253–1261, 2001.
- 1143 Lewis, T. R., Blitz, M. A., Heard, D. E., and Seakins, P. W. Direct evidence for a substantive reaction between the Criegee
1144 intermediate, CH₂OO, and the water vapour dimer, *Phys. Chem. Chem. Phys.*, 17, 4859–4863, 2015.
- 1145 Lin, L.-C., Chang, H., Chang, C., Chao, W., Smith, M. C., Chang, C., Lin, J. J., and Takahashi, K. Competition between H₂O
1146 and (H₂O)₂ reactions with CH₂OO/CH₃CHOO, *Phys. Chem. Chem. Phys.*, 18, 4557–4568, 2016.
- 1147 Long, B., Bao, J. L., and Truhlar, D. G.: Rapid unimolecular reaction of stabilized Criegee intermediates and implications for
1148 atmospheric chemistry, *Nat. Commun.*, 10, doi:10.1038/s41467-019-09948-7, 2019.
- 1149 Ma, Y., and Marston G.: Multifunctional acid formation from the gas-phase ozonolysis of β-pinene, *Phys. Chem. Chem. Phys.*,
1150 10, 6115–6126, 2008.
- 1151 Ma, Y., and Marston G.: Formation of organic acids from the gas-phase ozonolysis of terpinolene, *Phys. Chem. Chem. Phys.*,
1152 11, 4198–4209, 2009.
- 1153 Martinez, R. I. and Herron, J. T.: Stopped-flow studies of the mechanisms of alkene-ozone reactions in the gas-phase:
1154 tetramethylethylene, *J. Phys. Chem. A*, 91, 946–953, 1987.
- 1155 Mauldin, R. L., Berndt, T., Sipilä, M., Paasonen, P., Petäjä, T., Kim, S., Kurtén, T., Stratmann, F., Kerminen, V.-M., and
1156 Kulmala, M.: A new atmospherically relevant oxidant of sulphur dioxide, *Nature*, 488, 193–196, doi:10.1038/nature11278,
1157 2012.
- 1158 Neeb, P., Horie, O., and Moortgat, G. K. The nature of the transitory product in the gas-phase ozonolysis of ethene, *Chem.*
1159 *Phys. Lett.*, 37, 150-156, 1995.
- 1160 Neeb, P., Horie, O., and Moortgat, G. K. Formation of secondary ozonides in the gas-phase ozonolysis of simple alkenes,
1161 *Tetrahedron Lett.*, 246, 9297-9300, 1996.
- 1162 Neeb, P., Sauer, F., Horie, O., and Moortgat, G. K. Formation of hydroxymethyl hydroperoxide and formic acid
1163 in alkene ozonolysis in the presence of water vapour, *Atmos. Environ.*, 31, 1417-1423, 1997.
- 1164 Newland, M. J., Rickard, A. R., Alam, M. S., Vereecken, L., Muñoz, A., Ródenas, M., and Bloss, W. J.: Kinetics of stabilised
1165 Criegee intermediates derived from alkene ozonolysis: reactions with SO₂, H₂O and decomposition under boundary layer
1166 conditions, *Phys. Chem. Chem. Phys.*, 17, 4076–4088, 2015.
- 1167 Newland, M. J., Rickard, A. R., Sherwen, T., Evans, M. J., Vereecken, L., Muñoz, A., Ródenas, M., and Bloss, W. J.: The
1168 atmospheric impacts of monoterpene ozonolysis on global stabilised Criegee intermediate budgets and SO₂ oxidation:
1169 experiment, theory and modelling, *Atmos. Chem. Phys.*, 18, 6095-6120, 2018.
- 1170 Newland, M. J., Nelson B. S., Muñoz, A., Ródenas, M., Vera, T., Tarrega, J., and Rickard, A. R.: Trends in stabilisation of
1171 Criegee intermediates from alkene ozonolysis, *Phys. Chem. Chem. Phys.*, 22, 13698-13706, 2020.
- 1172 Nguyen, T. L., Winterhalter, R., Moortgat, G., Kanawati, B., Peeters, J., and Vereecken, L.: The gas-phase ozonolysis of β-
1173 caryophyllene (C₁₅H₂₄). Part II: A theoretical study, *Phys. Chem. Chem. Phys.*, 11, 4173–4183, 2009a.
- 1174 Nguyen, T. L., Peeters, J., and Vereecken, L.: Theoretical study of the gas-phase ozonolysis of β-pinene (C₁₀H₁₆), *Phys. Chem.*
1175 *Chem. Phys.*, 11, 5643-5656, 2009b.
- 1176 Nguyen, T. L., Lee, H., Matthews, D. A., McCarthy, M. C., and Stanton, J. F.: Stabilization of the Simplest Criegee
1177 Intermediate from the Reaction between Ozone and Ethylene: A High-Level Quantum Chemical and Kinetic Analysis of
1178 Ozonolysis, *J. Phys. Chem. A*, 119, 5524–5533, 2015.
- 1179 Nguyen, T. B., Tyndall, G. S., Crouse, J. D., Teng, A. P., Bates, K. H., Schwantes, R. H., Coggon, M. M., Zhang, L., Feiner,
1180 P., and Miller, D. O.: Atmospheric fates of Criegee intermediates in the ozonolysis of isoprene, *Phys. Chem. Chem. Phys.*, 18,
1181 10241–10254, 2016.
- 1182 Niki, H., Maker, P. D., Savage, C. M., Breitenbach, L. P., and Hurley, M. D. FTIR spectroscopic study of the mechanism for
1183 the gas-phase reaction between ozone and tetramethylethylene, *J. Phys. Chem. A*, 91, 941–946, 1987.



- 1184 O'Dwyer, M. A., Carey, T. J., Healy, R. M., Wenger, J. C., Picquet-Varrault, B., and Doussin, J. F.: The Gas-phase Ozonolysis
1185 of 1-Penten-3-ol, (Z)-2-Penten-1-ol, and 1-Penten-3-one: Kinetics, Products and Secondary Organic Aerosol Formation, *Z.*
1186 *Phys. Chem.*, 224, 1059–1080, 2010.
- 1187 O'Neal, H. E., and Blumstein, C.: A new mechanism for gas phase ozone-olefin reactions, *Int. J. Chem. Kinet.*, 5, 397-413,
1188 1973.
- 1189 Olzmann, M., Kraka, E., Cremer, D., Gutbrod, R., and Anderson, S.: Energetics, Kinetics, and Product Distributions of the
1190 Reactions of Ozone with Ethene and 2,3-Dimethyl-2-butene, *J. Phys. Chem. A*, 101, 9421–9429, 1997.
- 1191 Orzechowska, G. E., and Paulson, S. E.: Production of OH radicals from the reactions of C₄-C₆ internal alkenes and styrenes
1192 with ozone in the gas phase, *Atmos. Environ.*, 36, 571-581, 2002.
- 1193 Ouyang, B., McLeod, M. W., Jones, R. L., and Bloss, W. J.: NO₃ radical production from the reaction between the Criegee
1194 intermediate CH₂OO and NO₂, *Phys. Chem. Chem. Phys.*, 15, 17070-17075, 2013.
- 1195 Paulson, S. E., and Orlando, J. J. The reactions of ozone with alkenes: An important source of HO_x in the boundary layer,
1196 *Geophys. Res. Letts.*, 23, 3727-3730, 1996.
- 1197 Peltola, J., Seal, P., Inkilä, A., and Eskola, A.: Time-resolved, broadband UV-absorption spectrometry measurements of
1198 Criegee intermediate kinetics using a new photolytic precursor: unimolecular decomposition of CH₂OO and its reaction with
1199 formic acid, *Phys. Chem. Chem. Phys.*, 22, 11797-11808, 2020.
- 1200 Percival, C. J., Welz, O., Eskola, A. J., Savee, J. D., Osborn, D. L., Topping, D. O., Lowe, D., Utembe, S. R., Bacak, A.,
1201 McFiggans, G., Cooke, M. C., Xiao, P., Archibald, A. T., Jenkin, M. E., Derwent, R. G., Riipinen, I., Mok, D. W. K., Lee, E.
1202 P. F., Dyke, J. M., Taatjes, C. A., and Shallcross, D. E.: Regional and global impacts of Criegee intermediates on atmospheric
1203 sulphuric acid concentrations and first steps of aerosol formation, *Faraday Discuss.*, 165, 45–
1204 73, <https://doi.org/10.1039/C3FD00048F>, 2013.
- 1205 Pfeifle, M., Ma, Y. -T., Jasper, A. W., Harding, L. B., Hase, W. L., and Klippenstein, S. J.: Nascent energy distribution of the
1206 Criegee intermediate CH₂OO from direct dynamics calculations of primary ozonide dissociation, *J. Chem. Phys.*, 148, 174306,
1207 2018.
- 1208 Picquet-Varrault, B., Scarfoglierio, M., and Doussin, J. -F.: Atmospheric Reactivity of Vinyl Acetate: Kinetic and Mechanistic
1209 Study of Its Gas-Phase Oxidation by OH, O₃, and NO₃, *Environ. Sci. Technol.*, 44, 4615–4621, 2010.
- 1210 Pierce, J. R., Evans, M. J., Scott, C. E., D'Andrea, S. D., Farmer, D. K., Swietlicki, E., and Spracklen, D. V.: Weak global
1211 sensitivity of cloud condensation nuclei and the aerosol indirect effect to Criegee + SO₂ chemistry, *Atmos. Chem. Phys.*, 13,
1212 3163–3176, <https://doi.org/10.5194/acp-13-3163-2013>, 2013.
- 1213 Pinelo, L., Gudmundsdottir, A. D., and Ault, B. S.: Matrix Isolation Study of the Ozonolysis of 1,3- and 1,4-Cyclohexadiene:
1214 Identification of Novel Reaction Pathways, *J. Phys. Chem. A*, 117, 4174–4182, 2013.
- 1215 Raghunath, P., Lee, Y. -P., Lin, M. C.: Computational chemical kinetics for the reaction of Criegee intermediate CH₂OO with
1216 HNO₃ and its catalytic conversion to OH and HCO, *J. Phys. Chem. A*, 121, 3871–3878, 2017.
- 1217 Rathman, W. C. D., Claxton, T. A., Rickard, A. R., Marston, G. A theoretical investigation of OH formation in the gas-phase
1218 ozonolysis of *E*-but-2-ene and *Z*-but-2-ene, *Phys. Chem. Chem. Phys.*, 1, 3981-3985, 1999.
- 1219 Reissell, A., Harry, C., Aschmann, S. M., Atkinson, R., and Arey, J.: Formation of acetone from the OH radical- and O₃-
1220 initiated reactions of a series of monoterpenes, *J. Geophys. Res.*, 104, 13869–13879, 1999.
- 1221 Rickard, A. R., Johnson, D., McGill, C. D., and Marston, G. OH Yields in the Gas-Phase reactions of Ozone with Alkenes, *J.*
1222 *Phys. Chem. A*, 103, 7656–7664, 1999.
- 1223 Sakamoto, Y., Inomata, S., and Hirokawa, J.: Oligomerization Reaction of the Criegee Intermediate Leads to Secondary
1224 Organic Aerosol Formation in Ethylene Ozonolysis, *J. Phys. Chem. A*, 117, 12912–12921, 2013.
- 1225 Saunders, S. M., Jenkin, M. E., Derwent, R. G., and Pilling, M. J.: Protocol for the development of the Master Chemical
1226 Mechanism, MCM v3 (Part A): Tropospheric degradation of non-aromatic volatile organic compounds, *Atmos. Chem. Phys.*,
1227 3, 161-180, 2003.



- 1228 Sheps, L., Scully, A. M., and: UV absorption probing of the conformer-dependent reactivity of a Criegee intermediate
1229 CH₃CHOO Phys. Chem. Chem. Phys., 16, 26701-26706, 2014.
- 1230 Sheps, L., Rotavera, B., Eskola, A. J., Osborn, D. L., Taatjes, C., Au, K., Shallcross, D. E., Khan, M. A. H., Percival, C. J.
1231 The reaction of Criegee intermediate CH₂OO with water dimer: Primary products and atmospheric impact, Phys. Chem. Chem.
1232 Phys., 19, 21970-21979, 2017.
- 1233 Sipilä, M., Jokinen, T., Berndt, T., Richters, S., Makkonen, R., Donahue, N. M., Mauldin III, R. L., Kurtén, T., Paasonen, P.,
1234 Sarnela, N., Ehn, M., Junninen, H., Rissanen, M. P., Thornton, J., Stratmann, F., Herrmann, H., Worsnop, D. R., Kulmala, M.,
1235 Kerminen, V.-M., and Petäjä, T.: Reactivity of stabilized Criegee intermediates (sCIs) from isoprene and monoterpene
1236 ozonolysis toward SO₂ and organic acids, Atmos. Chem. Phys., 14, 12143-12153, 2014.
- 1237 Smith, M. C., Chao, W., Takahashi, K., Boering, K. A., and Lin, J. J. -M.: Unimolecular Decomposition Rate of the Criegee
1238 Intermediate (CH₃)₂COO Measured Directly with UV Absorption Spectroscopy, J. Phys. Chem. A, doi:
1239 10.1021/acs.jpca.5b12124, 2016.
- 1240 Stephenson, T. A., and Lester, M. I.: Unimolecular decay dynamics of Criegee intermediates: Energy-resolved rates, thermal
1241 rates, and their atmospheric impact, Int. Rev. Phys. Chem., 39, 1-33, 2020.
- 1242 Stone, D., Blitz, M., Daubney, L., Howes, N. U. M., and Seakins, P.: Kinetics of CH₂OO reactions with SO₂, NO₂, NO, H₂O,
1243 and CH₃CHO as a function of pressure, Phys. Chem. Chem. Phys., 16, 1139-1149, 2014.
- 1244 Stone, D., Au, K., Sime, S., Medeiros, D. J., Blitz, M., Seakins, P., Decker, Z., and Sheps, L.: Unimolecular decomposition
1245 kinetics of the stabilised Criegee intermediates CH₂OO and CD₂OO, Phys. Chem. Chem. Phys., 20, 24940-24954, 2018.
- 1246 Taatjes, C. A., Welz, O., Eskola, A. J., Savee, J. D., Scheer, A. M., Shallcross, D. E., Rotavera, B., Lee, E. P. F., Dyke, J. M.,
1247 Mok, D. K. W., Osborn, D. L., and Percival, C. J.: Direct Measurements of Conformer-Dependent Reactivity of the Criegee
1248 Intermediate CH₃CHOO, Science, 340, 177-180, 2013.
- 1249 Tadayon S. V., Foreman, E. S., and Murray, C.: Kinetics of the reactions between the Criegee intermediate CH₂OO and
1250 alcohols, J. Phys. Chem. A, 122, 258-268, 2018.
- 1251 Thiault, G., Thévenet, R., Mellouki, A., and Le Bras, G.: OH and O₃-initiated oxidation of ethyl vinyl ether, Phys. Chem.
1252 Chem. Phys., 4, 613-619, 2002.
- 1253 Tuazon, E. C., Aschmann, S. M., Arey, J., and Atkinson, R.: Products of the Gas-Phase Reactions of O₃ with a Series of
1254 Methyl-Substituted Ethenes, *Environ. Sci. Technol.*, 31, 10, 3004-3009, 1997.
- 1255 Vansco, M. F., Caravan, R. L., Zuraski, K., Winiberg, F. A. F., Au, K., Trongsiwat, N., Walsh, P. J., Osborn, D. L. Percival,
1256 C. J., Khan, M. A. H., Shallcross, D. E., Taatjes, C. A., and Lester, M. I.: Experimental Evidence of Dioxole Unimolecular
1257 Decay Pathway for Isoprene-Derived Criegee Intermediates, J. Phys. Chem. A, 124, 3542-3554, 2020.
- 1258 Vereecken, L., and Francisco, J. S.: Theoretical studies of atmospheric reaction mechanisms in the troposphere, Chem. Soc.
1259 Rev., 41, 6259-6293, 2012.
- 1260 Vereecken, L., Novelli, A., and Taraborrelli, D.: Unimolecular decay strongly limits the atmospheric impact of Criegee
1261 intermediates, Phys. Chem. Chem. Phys., 19, 31599-31612, 2017.
- 1262 Vereecken, L.: The reaction of Criegee intermediates with acids and enols, Phys. Chem. Chem. Phys., 19, 28630-28640, 2017.
- 1263 Vereecken, L., and Nguyen, H. M. T.: Theoretical Study of the Reaction of Carbonyl Oxide with Nitrogen Dioxide: CH₂OO
1264 + NO₂, Int. J. Chem. Kinet., 49, 752-760, 2017.
- 1265 Vereecken, L., Aumont, B., Barnes, I., Bozzelli, J., Goldman, M., Green, W., Madronich, S., Megillen, M., Mellouki, A.,
1266 Orlando, J., Picquet-Varrault, B., Rickard, A., Stockwell, W., Wallington, T., and Carter, W.: Perspective on Mechanism
1267 Development and Structure-Activity Relationships for Gas-Phase Atmospheric Chemistry. Int. J. Chem. Kinet., 50, 435-469,
1268 <https://doi-org.insu.bib.cnrs.fr/10.1002/kin.21172>, 2018.
- 1269 Vichiatti, R. M., Keidel Spada, R. F., Ferreira da Silva, A. B., Correto Machado, F. B., and Andrade Haiduke, R. L.: Accurate
1270 Calculations of Rate Constants for the Forward and Reverse H₂O + CO ↔ HCOOH Reactions, Chemistry Select, 2, 7267-
1271 7272, 2017.



- 1272 Viero, L.: Kinetics and mechanisms for the oxidation of unsaturated organic acids and esters under atmospheric conditions,
1273 Ph.D. Thesis, University College Dublin, 2008.
- 1274 Wadt, W. R., and Goddard, W. A.: The electronic structure of the Criegee intermediate. Ramifications for the mechanism of
1275 ozonolysis, *J. Am. Chem. Soc.*, 97, 3004-3021, 1975.
- 1276 Wang, J., Zhou, L., Wang, W., and Ge, M.: Gas-phase reaction of two unsaturated ketones with atomic Cl and O₃: kinetics
1277 and products, *Phys. Chem. Chem. Phys.*, 17, 12000–12012, 2015.
- 1278 Watson N. A. I., Black, J. A., Stonelake, T. M., Knowles, P. J., Beames, J. M.: An extended computational study of Criegee
1279 intermediate-alcohol reactions, *J. Phys. Chem. A*, 123, 218-229, 2019.
- 1280 Watson, N. A. I.: An Analysis of the Sources and Sinks for Criegee Intermediates: An Extended Computational Study, Ph.D.
1281 Thesis, University of Cardiff, <http://orca.cardiff.ac.uk/id/eprint/144742>, October 2021.
- 1282 Weidman, J. D., Allen, R. T., Moore, K. B., and Schaefer, H. F.: High-level theoretical characterization of the vinoxy radical
1283 ($\cdot\text{CH}_2\text{CHO}$) + O₂ reaction. *J. Chem. Phys.*, 148, 184308, 2018.
- 1284 Welz, O., Savee, J. D., Osborn, D. L., Vasu, S. S., Percival, C. J., Shallcross, D. E., and Taatjes, C. A.: Direct Kinetic
1285 Measurements of Criegee Intermediate (CH₂OO) Formed by Reaction of CH₂I with O₂, *Science*, 335, 204–207, 2012.
- 1286 Welz, O., Eskola, A. J., Sheps, L., Rotavera, B., Savee, J. D., Scheer, A. M., Osborn, D. L., Lowe, D., Murray Booth, A., Xiao,
1287 P., Anwar H., Khan, M., Percival, C. J., Shallcross, D. E., and Taatjes, C. A.: Rate coefficients of C1 and C2 Criegee
1288 intermediate reactions with formic and acetic acid near the collision limit: direct kinetics measurements and atmospheric
1289 implications, *Angew. Chem. Int. Ed. Engl.*, 53, 4547–4750, 2014.
- 1290 Winterhalter, R., Neeb, P., Grossmann, D., Kolloff, A., Horie, O. and Moortgat, G.: Products and mechanism of the gas phase
1291 reaction of ozone with β -pinene. *Journal of Atmospheric Chemistry*, 35(2), 165-197, 2000.
- 1292 Winterhalter, R., Herrmann, F., Kanawati, B., Nguyen, T. L., Peeters, J., Vereecken, L., and Moortgat, G.: The gas-phase
1293 ozonolysis of β -caryophyllene (C₁₅H₂₄). Part I: an experimental study, *Phys. Chem. Chem. Phys.*, 11, 4152–4172, 2009.
- 1294 Wennberg, P. O., Bates, K. H., Crouse, J. D., Dodson, L. G., McVay, R. C., Mertens, L. A., Nguyen, T. B., Praske, E.,
1295 Schwantes, R. H., and Smarte, M. D.: Gas-phase reactions of isoprene and its major oxidation products, *Chem. Rev.*, 118,
1296 3337–3390, <https://doi.org/10.1021/acs.chemrev.7b00439>, 2018.
- 1297 Wolff, S., Boddenberg, A., Thamm, J., Turner, W. V., and Gräb, S. Gas-phase ozonolysis of ethene in the presence of carbonyl-
1298 oxide scavengers, *Atmos. Environ.*, 31, 2965-2969, 1997.
- 1299 Yu, J. Z., Cocker, D. R., Griffin, R. J., Flagan, R. C., and Seinfeld, J. H.: Gas-phase ozone oxidation of monoterpenes: Gaseous
1300 and particulate products, *J. Atmos. Chem.*, 34, 207–258, 1999.
- 1301 Zhao, Y., Wingen, L. M., Perraud, V., Greaves, J., and Finlayson-Pitts, B. J.: Role of the reaction of stabilized Criegee
1302 intermediates with peroxy radicals in particle formation and growth in air, *Phys. Chem. Chem. Phys.*, 17, 12500–12514, 2015.
- 1303 Zhou, S., Barnes, I., Zhu, T., Klotz, B., Albu, M., Bejan, I., and Benter, T.: Product Study of the OH, NO₃, and O₃ Initiated
1304 Atmospheric Photooxidation of Propyl Vinyl Ether, *Environ. Sci., Technol.*, 2006.
- 1305 Zhou, S.: Atmospheric Oxidation of Vinyl Ethers, PhD thesis, Bergische Universität Wuppertal, 2007.
- 1306 Ziemann, P. J.: Evidence for Low-Volatility Diacyl Peroxides as a Nucleating Agent and Major Component of Aerosol Formed
1307 from Reactions of O₃ with Cyclohexene and Homologous Compounds, *J. Phys. Chem. A*, 106, 4390–4402, 2002.
- 1308